SAE Toolbox

Final Design Report

Derek Griffith, Logistics Manager, Prototype Engineer

Hailey Hein, Project Manager, CAD Engineer, Financial Manager

Haoran Li, Test Engineer

Yanbo Wang, Manufacturing Engineer

Summer 2025-Fall 2025

Project Sponsor: NAU SAE

Faculty Advisor: David Willy

Instructor: Carson Pete

DISCLAIMER

This report was prepared by students as part of a university course requirement. While considerable effort has been put into the project, it is not the work of licensed engineers and has not undergone the extensive verification that is common in the profession. The information, data, conclusions, and content of this report should not be relied on or utilized without thorough, independent testing and verification. University faculty members may have been associated with this project as advisors, sponsors, or course instructors, but as such they are not responsible for the accuracy of results or conclusions.

EXECUTIVE SUMMARY

The SAE Toolbox Capstone Project, undertaken by a team of Northern Arizona University (NAU) engineering students, addresses the needs of the NAU SAE Formula and Baja Teams by designing and manufacturing a robust, multifunctional toolbox cart for use in competition pits and shop environments. Initiated in Summer 2025 and continuing through Fall 2025, the project responds to client requirements for a mobile, durable, and efficient cart capable of supporting race-day operations and year-round shop use. Key customer requirements include maneuverability on uneven terrain, organized storage for tools and equipment, a secure fire extinguisher mount, onboard power for charging tools, and single-person operability. The project, sponsored by NAU SAE and advised by Dr. David Willy, has a budget of $2,000, with a projected $1,372.06 spent to date, bolstered by a fully sponsored $1,150 base frame and a $501 sponsorship from Findlay Toyota Flagstaff.

The final design, selected through a rigorous concept generation and evaluation process, is a 60" x 30" x 35" cart constructed from 1" square steel tubing, featuring four 10-inch off-road casters for enhanced mobility. A pallet truck-style steering handle with a tie rod system ensures a tight 31.3-inch turning radius, validated through SolidWorks motion studies. The cart includes a five-drawer locking toolbox for organized storage, a chain-assisted tire storage compartment, a fire extinguisher mount, and a dedicated space for a power supply (currently under evaluation, with a Power Smart 2500W inverter generator as a leading option). A disc brake system with a rotor and caliper ensures secure stopping on uneven terrain. Additional features, such as a bench-mounted vice and sponsor branding areas, enhance functionality and stakeholder engagement. The design meets engineering requirements, including a 500-pound load capacity with a safety factor of two, a maximum 50-pound push force on a five-degree incline, and tilt stability up to a ten-degree lateral incline.

Major results include successful validation of the steering system through CAD motion studies, confirming adequate maneuverability for pit and trailer environments. Finite Element Analysis (FEA) is ongoing to verify the structural integrity of the frame and tire carrier, with initial simulations indicating that steel components are necessary for high-stress areas to ensure durability. Prototyping efforts have focused on the steering and brake systems, with plans for further testing to validate drawer locking mechanisms and loaded weight performance. Future tests will include hill-stopping, mock tech inspections, and maneuverability assessments under a 500-pound load to ensure single-user operability and reliability in real-world conditions. The project remains on track to deliver a fully functional, field-tested pit cart by the end of Fall 2025, accompanied by a comprehensive SolidWorks CAD model, technical drawings, and sponsor recognition materials, ensuring alignment with both client expectations and course requirements.

Table of Contents

1 BACKGROUND

This chapter provides an overview of the SAE Toolbox Capstone Project by summarizing the project's origin, goals, and context. Section 1.1 outlines the project description, including client expectations and financial targets for sponsorship and fundraising. Section 1.2 defines the key deliverables that will be completed over the course of the project to meet both course and client requirements. Section 1.3 establishes the success metrics that will be used to evaluate the project, including both qualitative and quantitative performance indicators. Together, these sections form the foundation for understanding the scope, intent, and expectations of the project moving forward.

1.1 Project Description

This project was initiated in response to a request from the NAU SAE Formula and Baja Teams to design and manufacture a robust, multifunctional toolbox cart for use in competition pits and shop spaces. In meetings with the teams and faculty sponsor Dr. David Willy, specific needs were identified including mobility over rough terrain, organized tool and equipment storage, fire extinguisher housing, and the ability to charge onboard batteries and devices. The goal is to streamline operations during competition and optimize shop efficiency year-round.

Budget and fundraising efforts have been directed toward securing both monetary and material sponsorship. The target fundraising is $1,000, with sponsorship tiers developed to encourage industry and local business contributions, including Copper ($50–$200), Silver ($201–$500) and Gold ($501–$1000).

1.2 Deliverables

The major deliverables for the SAE Toolbox project are aimed at meeting both course requirements and client expectations, while also supporting the competitive needs of the NAU Formula and Baja SAE team. By the end of Fall 2025, the team will deliver a fully functional and field-tested pit cart designed specifically for rugged, off-road use. Accompanying this physical delivery will be a comprehensive SolidWorks CAD model, complete with technical drawings for all parts and assemblies. To verify structural integrity and functionality, Finite Element Analysis (FEA) simulations will be conducted and documented. A detailed cost breakdown will be provided, along with sponsor recognition materials such as engraved nameplates or branded stickers applied to the final product. In addition to the physical and digital assets, the team will present their work in formal design reviews, in-class ME 476C and 486C presentations, and to the SAE Formula and Baja teams to ensure alignment with all stakeholder expectations.

1.3 Success Metrics

Success for the SAE Toolbox project—intended to support both the Baja and Formula SAE teams at NAU—will be measured by its ability to meet or exceed all customer requirements while performing reliably in demanding pit and off-road environments. Key success metrics include the cart's ability to withstand terrain testing without any functional failures or structural damage, and its ability to pass tilt and balance assessments while fully loaded with tools, tires, and racing equipment. Additionally, the toolbox must fit within space constraints typical of competition pit areas and allow safe, immediate access to critical items such as power tools and fire extinguishers. User satisfaction will also be a major indicator of success, evaluated through direct feedback from team members after hands-on testing. These performance metrics will be validated through a combination of SolidWorks FEA and motion simulations, relevant engineering calculations (such as axle loading and moment balancing), physical prototype testing, and usability evaluations conducted in real-world pit scenarios.

2 REQUIREMENTS

This chapter defines the performance and design expectations for the SAE Toolbox Capstone Project. Section 2.1 outlines the customer requirements gathered through meetings with the SAE Formula and Baja Teams, capturing the needs and preferences of the end users. Section 2.2 translates those needs into quantifiable engineering requirements, each with specific units and target values that guide the design. Section 2.3 presents the House of Quality (HOQ), which maps the relationships between customer and engineering requirements, prioritizes design focus areas, and incorporates benchmarking data. Together, these sections ensure that the project is rooted in clear, measurable objectives aligned with customer goals.

2.1 Customer Requirements (CRs)

The customer requirements for the SAE Toolbox reflect the needs of both the Baja and Formula SAE teams and are focused on functionality, safety, and usability in off-road and pit environments. First and foremost, the cart must be maneuverable on uneven surfaces such as gravel and grass, ensuring it can be transported to and around the competition site with ease. It must also provide ample storage for SAE-specific tools and spare parts, allowing quick access during repairs and adjustments. A locked compartment is required to secure high-value tools and equipment when unattended. Additionally, the design must integrate a standard ten-pound fire extinguisher in an accessible and secure mount. To support the team's workflow, the cart should include an onboard battery or charging capability for power tools. Visual representation of team sponsors is also important, so space for logos or branded stickers should be incorporated. Finally, the entire system should be operable by a single person, minimizing labor requirements and improving overall efficiency during competitions.

2.2 Engineering Requirements (ERs)

The SAE Toolbox design translates customer needs into measurable constraints for real-world performance. For off-road use, it must have rubber wheels at least 6" in diameter (ideally 8–10") for traction and shock absorption. A single user must operate it with ≤50 lb. of force on a 5° incline when fully loaded. Storage must include a 3'×2'×1' gear compartment and drawers for tools like brake bleed kits. A lockable compartment is required, with a latch that withstands 100 lb. of pull force. The toolbox must mount a standard 10 lb. fire extinguisher and power supply for charging. Its footprint must stay within 30"×60" to fit trailers. Structurally, the frame must support 500 lb. with a safety factor of 2 (verified by FEA) and remain stable on a 10° lateral incline.

2.3 House of Quality (HoQ)

The House of Quality (HoQ) is a key early-stage tool in the SAE Toolbox project, translating customer needs into measurable engineering requirements. It maps features such as maneuverability, storage, stability, power, and single-user operation to metrics such as caster size, internal volume, safety factor, and push force. The matrix also includes benchmarking, target values, and correlation strengths to guide design priorities and resource allocation. A full-resolution HoQ with engineering links, difficulty ratings, and competitor analysis is included below.

House of Quality — Roof (Technical Requirements Correlations)

Technical Requirement	Correlation values
Rubber Casters 6" to 10"	
Integrated manual steering	9
Hand Braking/ Locking Wheels	9, 9
Acceptable Volumetric Footprint in Trailer	
Locking Drawers	6
3'x2'x1' Volume for Driver bag	6
Fire Extinguisher Mount	
Integrated Power System for Tools	
Charging Capability	9
Powered Tools Storage	6, 3, 9
Sound System (optional)	
Mounting locations for vice, arbor press, etc	6
Shade	6
Welded Aluminum frame with bolted accessories	3, 3, 3
Storage for saftey equipment, brake bleed kit, saftey wire puller.	6, 9

Legend

A	Redline 75" Pit Cart
B	Winter Pit Products
C	DK Hardware

Technical Requirements / Customer Opinion Survey

Customer Needs	Customer Weights	Rubber Casters 6" to 10"	Integrated manual steering	Hand Braking/ Locking Wheels	Acceptable Volumetric Footprint in Trailer	Locking Drawers	3'x2'x1' Volume for Driver bag	Fire Extinguisher Mount	Integrated Power System for Tools	Charging Capability	Powered Tools Storage	Sound System (optional)	Mounting locations for vice, arbor press, etc	Shade	Welded Aluminum frame with bolted accessories	Storage for saftey equipment, brake bleed kit, saftey wire puller.	1 Poor	2	3 Acceptable	4	5 Excellent
Large Toolbox	4	6	3	6	9	9					6		3		6	3			B		AC
Hold all of driver equipment/ spare wheels + rims	4	6			9		9												AC		B
Mounted items (arbor press, vice, grinding wheel,etc)	4	3			9				3	6	9		9						AC	B	
Price	5	3	3								3		6		6	3	ABC				
Brakes/ steering/ 6-10 inch casters	4	9	9	9															B		AC
Technical Requirement Units		inch	N/A	lbf/ N	ft^3	N/A	ft^3	N/A	Watts	Watts	ft^3	N/A	N/A	ft^3	ft^3	ft^3					
Technical Requirement Targets		10 in	Y	2+	72 ft^3	Y	6 ft^3	Y			2ft^3	Y	3 locations	72 ft^3	Y	2 ft^3					
Absolute Technical Importance		50	50	50	50	30	50	50	30	30	50	10	50	50	50	30	Total Score				
Relative Technical Importance		8%	8%	8%	8%	5%	8%	8%	5%	5%	8%	2%	8%	5%	8%	5%	610				

Figure 1: House of Quality

3 Research Within Your Design Space

3.1 Benchmarking

To guide the SAE Toolbox design, we benchmarked three leading pit carts: the Redline 75" Mechanics Toolbox [1], Winter Pit Products Acceleration Cart [2], and Extreme Tools TXPIT7009BK [3]. These examples helped establish expectations for maneuverability, storage, and functionality.

The Redline 75" [1] offers a rugged, simple design with large casters and a wide storage base but lacks modularity or onboard power—features we aim to add. The Winter Acceleration Cart [2] stands out for its dual axle steering and flatbed layout, influencing our focus on off-road stability and control. The Extreme Tools TXPIT7009BK [3] includes integrated brakes, secure storage, and a stainless-steel work surface, directly shaping our approach to safety and organization.

Subsystem-level comparisons—such as caster sizes, drawer locks, and power integration—further informed our decisions. For instance, 6–10" casters were standard across models, supporting our wheel size choice. Winter's steering geometry and DK's locking system were key inspirations. These benchmarks define our design priorities and highlight innovation opportunities in modular storage, power access, and off-road capability.

3.2 Literature Review

3.2.1 Derek Griffith

[4] **Braking of Road Vehicles, Elsevier BV, 2022**

This volume provides foundational insights into braking systems, detailing mechanical, hydraulic, pneumatic, and electronic brakes, along with their performance characteristics. It discusses the heat dissipation, friction behavior, and stability aspects that are essential in selecting and designing safe and efficient braking systems. For the SAE tool cart project, this reference offers a solid technical foundation for choosing an appropriate braking mechanism, ensuring that the tool cart can manage various loads and provide consistent stopping power in dynamic environments.

[5] **Energy Storage Systems for Electric Vehicles, 2020**

This book explores the wide range of energy storage methods used in electric vehicles, such as lithium-ion batteries and ultracapacitors, and explains their integration into vehicular power and braking systems. Key topics like charge/discharge cycles, power management, and regenerative braking directly inform how to size and wire power systems efficiently. For the tool cart, this source supports the design of a self-contained electrical power system by providing guidance on storage selection and power delivery.

[6] **Model-Based Range Extension Control System for Electric Vehicles With Front and Rear Driving–Braking Force Distributions, Fujimoto & Harada, 2015**

This paper presents a model-based control system that dynamically distributes brake and driving forces between front and rear axles in electric vehicles, improving stability and extending battery range. This research can influence how force is applied to each wheel of the cart to prevent skidding and improve maneuverability on slick or uneven pit lane surfaces.

[7] **Optimal Allocation Method of Electric/Air Braking Force of High-Speed Train Considering Axle Load Transfer, Guo & He, 2024**

This study introduces a method for optimally allocating braking force between electric and pneumatic systems in high-speed trains, considering axle load transfer during deceleration. For the SAE tool cart, which may experience varying loads and shifting weight distribution due to tool placement or movement, understanding how to balance braking force can improve both safety and wear characteristics. This source helps justify braking layouts that compensate for uneven loading and provide stable, controlled stops.

[8] A New Model of Stopping Sight Distance of Curve Braking Based on Vehicle Dynamics, Xia et al., 2016

Xia et al. presents a refined model of stopping sight distance (SSD) by accounting for vehicle dynamics like lateral forces and curve radii, which traditional models often overlook. For the tool cart, which may need to navigate tight corners or stop on variable terrain in crowded areas, this study helps estimate realistic braking distances and informs safer design of the brake system and operator control logic. It can also support decisions about maximum allowable speed in operational scenarios.

[9] Fuzzy Scheduled Optimal Control of Integrated Vehicle Braking and Steering Systems, Mirzaei & Mirzaeinejad, 2017

This research develops a fuzzy logic-based control system that integrates braking and steering, enabling real-time adjustments to improve handling and stability under dynamic conditions. While advanced, the approach offers insight into how to coordinate steering and braking in a compact, maneuverable platform like the tool cart.

[10] R. G. Budynas, J Keith Nisbett, and Joseph Edward Shigley, Shigley's mechanical engineering design, 11th ed. New York, Ny: Mcgraw-Hill Education, 2020.

Shigley's Mechanical Engineering Design will be used as a foundational reference for analyzing both compression and extension springs in the mechanical design process. This text provides detailed methodologies for calculating spring forces which is critical when selecting or designing springs for reliable performance under dynamic loads.

[11] David Gordon Wilson, *Bicycling science*. Cambridge (Massachusetts): Mit Press, 2004.

Bicycling Science will serve as a key resource for understanding the principles of bicycle braking systems, which are similar if not identical to the brakes used by the toolbox. The book explores the physics behind braking dynamics, including friction, weight transfer, and stopping distances, which are essential when analyzing or designing effective braking mechanisms.

3.2.2 Hailey Hein

[12] "Vehicle Static Stability Factor," *Automotive Engineering Technical Article*, SAE International.

This article introduces the Static Stability Factor (SSF), calculated as track width divided by twice the center of gravity (CG) height. The SSF helps estimate rollover thresholds on inclined surfaces. This is highly applicable to our cart design since it must remain upright and stable during transport on uneven terrain. The SSF equation is directly usable during our early CAD-based layout and during CG-height sensitivity analysis.

[13] D. Raymer, *Aircraft Design: A Systems Engineering Approach*, American Institute of Aeronautics and Astronautics, 2012.

Though focused on aircraft, this book provides valuable principles regarding center of gravity placement, mass distribution, and static margin stability. These concepts apply to our cart's loaded condition, especially when storing heavy parts such as tools and wheels. It reinforces the need to keep CG as low and centered as possible in the CAD model.

[14] **A. T. Jones, "Tip-Over Stability of Mobile Boom Cranes," M.S. thesis, Dept. Mech. Eng., Purdue Univ., 2018.**

This thesis models tip-over hazards in mobile cranes under dynamic and static conditions. Though larger in scale, its methodology, especially the use of free-body diagrams and moment equations—is transferable to our cart. I will apply this to simulate corner-case loading, such as placing a vice or jack stand near one side.

[15] **J. Martinez and S. Kim, "Tip-Over Stability Using Dynamic Simulation,"** *J. of Field Robotics*, **vol. 33, no. 6, pp. 812–829, 2017.**

This paper describes multi-body simulation using MATLAB/ADAMS to evaluate orchard robot stability. It provides logic and modeling techniques for simulating movement across sloped or bumpy terrain. For our project, this supports the decision to use CAD motion simulation to visualize dynamic responses and test for critical angles of instability.

[16] **T. Kato and F. Miyazaki, "Analytic Solutions for Wheeled Mobile Manipulators,"** *IEEE Trans. on Robotics*, **vol. 20, no. 2, pp. 378–384, Apr. 2004.**

This research provides exact solutions for wheel loading and tipping force thresholds when vehicles operate on inclines. Its load distribution equations are useful for calculating expected axle forces during worst-case braking scenarios. These formulas will be integrated into the hand calculations that verify my CAD design.

[17] **Hamilton Caster Co., "Tipping Hazards in Tool Carts,"** *Hamilton Whitepaper*, **2021.**

This industry whitepaper outlines practical safety concerns in mobile carts, including poor weight distribution, undersized wheels, and sudden stops. It includes general recommendations for CG height, wheel spacing, and slope handling. These industry guidelines reinforce our design constraints and serve as sanity checks for my structural and stability choices.

[18] **S. Blake, "Crane Tipping Theory Using CAD,"** *Design World Case Study*, **2020.**

This article discusses how to simulate tipping and load transfer directly within CAD platforms like SolidWorks and Fusion 360. It provides step-by-step instruction for simulating moment arms, center of gravity shifts, and static balance using real design geometries. This will be directly applied in my CAD analysis of the frame and wheel layout.

[19] **P. Black and E. Adams, "Finite Element Analysis of Mobile Structures,"** *Mechanical Engineering Letters*, **vol. 14, no. 1, pp. 54–61, 2022.**

This paper explores stress and deformation in wheeled mobile frames under distributed and point loading. It presents FEA approaches ideal for analyzing the structural integrity of frame tubing—key for ensuring the cart's load-bearing capability meets our minimum safety factor.

3.2.3   Haoran Li

[20] **M. E. Cooper, "Rolling Resistance and Energy Losses in Manual Wheelchairs," Journal of Rehabilitation Research and Development, vol. 34, no. 3, pp. 289–298, 1997. (Paper)**

This article analyzes how wheel material and surface type affect rolling resistance due to hysteresis losses. The experimental data helps estimate the push force needed for rubber wheels, supporting our cart's maneuverability analysis and wheel selection.

[21] **"Rolling Resistance Coefficient Reference Table," The Engineering Toolbox. (Online)**

This webpage introduces the basic definition and formula of rolling resistance, $F_r = C_r * W$, and provides typical coefficient values for rubber, polyurethane, and steel wheels on various surfaces. These standardized values enable accurate estimation of rolling resistance for carts on different terrains, helping validate and refine the $F_r = C_r * W$ model. This supports performance evaluation of wheels and user effort estimation in our design.

[22] **D. Lippert and J. Spektor, Rolling Resistance and Industrial Wheels, Hamilton Caster White Paper No. 11, 2012. (Online)**

This white paper provides rolling resistance data for industrial wheels under various loads and surfaces. It introduces key influencing factors—wheel diameter, tread material, and floor roughness—and presents a calculation formula $F = f * \frac{w}{R}$. The content supports our toolbox design by guiding caster selection and push force estimation.

[23] **R. Zepeda, F. Chan, and B. Sawatzky, "The effect of caster wheel diameter and mass distribution on drag forces in manual wheelchairs," Journal of Rehabilitation Research and Development, vol. 53, no. 6, pp. 893–900, 2016. (Paper)**

This study investigates the effects of caster wheel diameter and load distribution on rolling resistance in manual wheelchairs. Experiments conducted using a treadmill and force sensors showed that small-diameter casters (4 inches) significantly increase resistance only when more than 40% of the total weight is placed over them. Weight distribution was found to have a greater impact on drag than wheel size. These findings support our toolbox design by emphasizing the importance of proper load placement and center-of-mass control to reduce push effort.

[24] **Z. Pomarat, T. Marsan, A. Faupin, Y. Landon, and B. Watier, "Wheelchair caster power losses due to rolling resistance on sports surfaces," *Disabil. Rehabil. Assist. Technol.*, vol. 20, no. 4, pp. 1176–1182, 2025. (Paper)**

This paper analyzes power losses from rolling resistance in different caster wheels under varying speeds, loads, and surfaces. It shows that caster type and floor material significantly affect energy loss, supporting caster selection decisions for improved toolbox mobility.

[25] **Darcor Ltd., *Guide to Designing Manual Materials Handling Carts – Selecting Casters, Reducing Workplace Injury*, 2018. (Book)**

This guide explains how caster diameter, material, and offset affect rolling resistance and push force. The "Caster Effects" section offers useful equations and design tips that support caster selection and handling performance in our toolbox project.

[26] **S. J. Khan, A. Ustun, and B. Venkatesh, Fundamentals of Smart Grid Systems, 1st ed., Elsevier, 2023, ch. 10. (Book)**

This chapter discusses the concept of rolling resistance and its impact on vehicle movement. It provides useful explanations for understanding how surface friction and load affect motion, which supports our toolbox design by helping evaluate caster performance under different loading conditions.

3.2.4   Yanbo Wang

This group of sources addresses practical power consumption parameters and efficiency considerations related to on-board electrical output systems, including AC outlets and USB interfaces.

[27] **Stanley Black & Decker, "DEWALT DCB112 12 V/20 V MAX Charger – Product Specification," DEWALT.com, accessed Jun. 2025.**

The spec sheet lists an AC input of 100–260 V and a peak draw of ≈ 80 W, giving a realistic figure-of-merit for one power-tool battery charger.

[28] **Greatatop, "UL-Certified 5 V 2 A (10 W) USB Wall Charger – Product Listing," Amazon Marketplace, 2024.**

Provides a concrete 10 W rating for a standard USB-A port, matching the 2 A@5 V assumption used in our load table.

[29] **M. Fedkin, "Efficiency of Inverters," EME 812 Utility Solar Power (Penn State Univ.), Lesson 6.5, 2024.**

States that high-quality pure-sine inverters achieve 90–95 % efficiency, while low-cost modified-sine models run 75–85 %; our 75 % system-loss factor adopts the conservative end of this range.

[30] **Battery University, "BU-403: Charging Lead Acid," BatteryUniversity.com, 2024.**

Notes overall charge/discharge efficiencies of 80–90 % for new VRLA batteries, validating the 90 % discharge-efficiency term in our calculations.

[31] **EnergySage, "Lithium-Ion vs. Lead-Acid Batteries – Efficiency & Cycle Life," EnergySage.com, 2023.**

Reports typical round-trip efficiencies: Li-ion ≈ 95 %, Lead-acid ≈ 80–85 %, supporting our chemistry-selection discussion and margin choices

[32] **USB Implementers Forum, "USB Power Delivery Revision 3.1 – Overview," usb.org, 2021.**

Defines USB-PD power profiles up to 240 W and confirms legacy USB-A/B ports remain limited to 5 V nominal, reinforcing the 10 W/port cap used here.

[33] **USB Implementers Forum, "USB 2.0 Specification," Release 2.0, Jun. 2025.**

Section 7.2.1 fixes VBUS at 4.75–5.25 V and 500 mA (2.5 W) for standard downstream ports; higher-current BC 1.2 charging logic scales to 1.5 A. Provides the regulatory ceiling for our USB-load envelope.

3.3 Mathematical Modeling

3.3.1 Brake Sub Assembly - Derek Griffith

The braking sub assembly will contain two calipers mounted on the front wheel hubs of the cart. The cables will be connected to the pull handle of the tool cart via a brake lever akin to a bicycle brake system. To calculate the braking force of the cart in motion, the following equations are required [32]:

1. **Cart Mass (loaded):**

$$m = 227 \text{ kg} \tag{1}$$

2. **Cart Velocity:**

$$v = 2 \text{ m/s} \tag{2}$$

3. **Stopping Distance:**

$$d = 3 \text{ m} \tag{3}$$

4. **Work:**

$$W = F \cdot d \tag{4}$$

5. **Kinetic Energy:**

$$E_k = \frac{1}{2} m v^2 \tag{5}$$

6. **Braking Force:**

$$F_b = \frac{1}{2} \frac{m v^2}{d} \tag{6}$$

Using eqn. (1), (2), (3), and (6):

$$F_b = \frac{1}{2} \frac{(227)(2)^2}{3} = 151.33 \, N \approx 34 \, lbf$$

This force of 34lbf is applied at the contact point between the road and the tire therefore, the actual required braking force will be higher due to the braking being applied to the disc, not the actual wheel itself. Since the wheel and brake rotor are connected, we can use the relation [32]:

$$F_{b1} * r_1 = F_{b2} * r_2 \tag{7}$$

Using eqn. (7) with a wheel radius of 5 in (0.127 m) and a rotor radius of 4 in (0.1016 m):

$$151.33 \, N * 0.127 \, m = F_b * 0.1016 \, m$$

$$F_b = 189.16 \, N \approx 43 \, lbf$$

It is important to note that while this is the required braking force for the cart for the velocity above, there is slipping between the brake rotor and the brake pad / piston. This coefficient of friction has been experimentally analyzed by David Gordon Wilson [11]. Based on his data and interpolating the data, we get a μ value of 0.238.

Compression Spring Method:
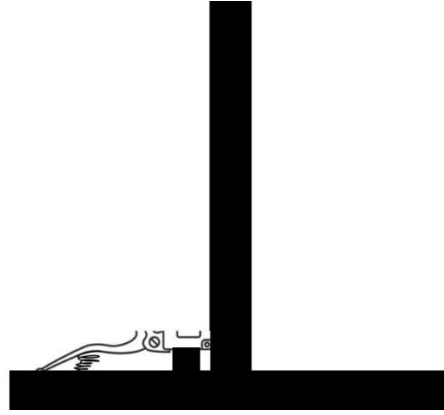
Figure 2: Compression Spring Brake Setup

For the sizing of hydraulic brakes for this special reversed brake system, the important part is the spring that will provide the constant braking force and the mechanical advantage (leverage ratio) at which the spring will act. The current mechanical advantage is estimated to be about 6 based on the available brake handle sizes. Using Shigley's Mechanical Engineering Design [10], an estimated spring ratio was calculated for the prototype:

$$k = \frac{d^4 G}{8 D^3 N} = \frac{\left(\frac{1}{8} in\right)^4 (11.5*10^6 \ psi)}{8\left(\frac{7}{8} in\right)^3 (13)} = 40.3 \ \text{lb/in} \tag{8}$$

The spring while under the brake handle was compressed by ¾ in. This means that the force acting on the brake lever is about 30.225 lbf. To calculate the pressure, we use:

$$P = \frac{F}{A} = \frac{6(30.225 \ lbf)}{\frac{\pi}{4}(0.4 \ in)^2} = 1443.14 \ psi \tag{9}$$

with 0.4 in. being the diameter of the piston. Then using the pressure applied to a $1 \ in^2$ brake pad, and with the coefficient of friction value we calculated earlier, we get an applied brake force of 344 lbf to the rotor.

Force on Casters During Braking:
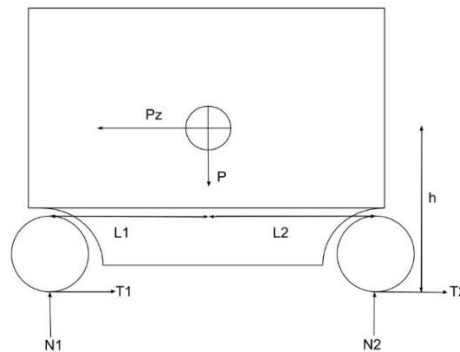
Figure 3: Toolbox FBD

During braking of the toolbox, the loading of the box will shift in the direction of motion / deceleration. The equations that describe the loading shift are:

$$N_1 = P\left[\frac{L_2}{(L_1+L_2)} + \frac{zh}{(L_1+L_2)}\right] \tag{10}$$

$$N_2 = P\left[\frac{L_1}{(L_1+L_2)} - \frac{zh}{(L_1+L_2)}\right] \tag{11}$$

The variable z where $z = \frac{J}{g}$ describes how the toolbox will decelerate compared to the acceleration due to gravity. From calculations in presentation 1, we found that:

$$J = \frac{\left(2\frac{m}{s}\right)^2}{2(3m)} = .667 \; m/s^2 \tag{12}$$

With an h value of approximately 2 ft off the ground, we see that the loads of N_1 and N_2 are:

$$N_1 = P\left[\frac{L_2}{(L_1 + L_2)} + \frac{zh}{(L_1 + L_2)}\right] = 174.06 \; kg \; \approx 384 \; lbs$$

$$N_2 = P\left[\frac{L_1}{(L_1 + L_2)} - \frac{zh}{(L_1 + L_2)}\right] = 52.94 \; kg \approx 117 \; lbs$$

Adding the two values we get our original 500lb load and notice that the deceleration end of the toolbox will experience about 77% of the loading.

3.3.2 Steering Sub Assembly – Hailey Hein

To find the necessary values for a turning radius calculation, I used the collision detection function in SolidWorks to make sure the turning assembly was at its maximum. From there, I used the measure tool to create a right triangle from the outside flat of the tire to the center of the assembly. This was repeated for both wheels in the instance of turning right. The following diagrams were derived.
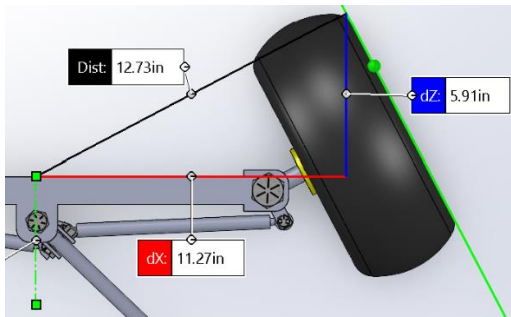
Figure 4: Inner Turned Wheel Geometry
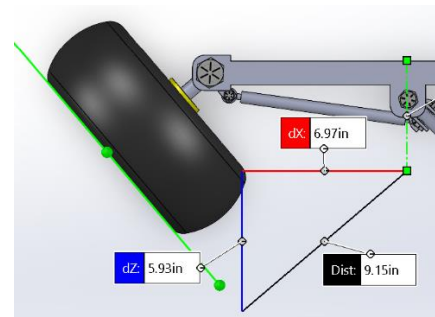
Figure 5: Outer Turned Wheel Geometry

With these measurements, I then did the right triangle calculations to find the angle that each wheel turns when the system is at its max. This value then influenced a turning radius calculation to see if this system will be able to maneuver within the enclosed trailers constraints and pit areas.

The tool cart exhibits turning behavior like a rear-axle-steered trolley, and its minimum turning radius can be estimated using geometric relationships between the wheelbase and track width. Using the triangle formed by the caster pivot axis and the wheel's path, I approximated the maximum steering angles of both the inside and outside tires.

Outside Tire Geometry:

- a = 5.93 in, b = 6.97 in, c = 9.15 in

Using basic trigonometry: [45]

- For angle α (wheel pivot angle relative to wheelbase line) :

$$\sin(\alpha) = a / c \text{ so } \alpha = \arcsin(a / c) = \arcsin(5.93 / 9.15) = 40.40\circ \tag{13}$$

- For angle β (wheel pivot angle relative to diagonal track offset):

$$\sin(\beta) = b / c \text{ so } \beta = \arcsin(b / c) = \arcsin(6.97 / 9.15) = 49.62\circ \tag{14}$$

Inside Tire Geometry:

- a = 5.91 in, b = 11.27 in, c = 12.73 in
- For angle α:

$$\sin(\alpha) = a / c \text{ so } \alpha = \arcsin(a / c) = \arcsin(5.91 / 12.73) = 27.66\circ \tag{15}$$

- For angle β:

$$\sin(\beta) = b / c \text{ so } \beta = \arcsin(b / c) = \arcsin(11.27 / 12.73) = 62.29\circ \tag{16}$$

These angles define how much each caster swivels from its neutral (0°) position during a tight turn. Notably, the outside tire rotates further than the inside, due to a larger lateral sweep required to maintain a tight circular path around the cart's center. This behavior is common in multi-caster systems, particularly when rear casters dominate steering input [44].

While the theoretical minimum turning radius approaches zero due to the 90° swivel range of the casters, real-world constraints (caster offset, geometry, wheel scrub, and swivel resistance) limit this.

Using a geometric approximation based on the cart's wheelbase and track width, the minimum turning radius (measured from the center of the turning circle to the midpoint between the rear wheels) can be estimated as: [46]

$$R_{min} = \frac{L}{2} + \frac{W}{2} * \cot(\theta_{max}) \tag{17}$$

Where:

- L = 49.77in (wheelbase),

- W = 24.75in (track width),

- θ max = 62.29∘ (maximum steering angle from β inside tire).

Measured directly from the CAD model. Then computing:

$$\cot(62.29) = \frac{1}{\tan(62.29)} = 0.5217 \tag{18}$$

$$R_{min} = \frac{62.29}{2} + \frac{27.66}{2} * 0.5217 = 38.36 \text{ in} \tag{19}$$

This produces the result that the minimum turning radius is approximately 38 inches. This means the cart can complete a 180° turn within a circular footprint of roughly in diameter, allowing tight maneuvers in confined spaces such as race pits or trailer interiors, which typically exceed 40 inches in width [42].

3.3.3 Cabinet Volume Sub Assembly – Hailey Hein

A key requirement of the tool cart is its ability to store essential equipment used during race events. To ensure the design meets this need, we identified the minimum required storage volume based on the dimensions of typical items carried by the team.
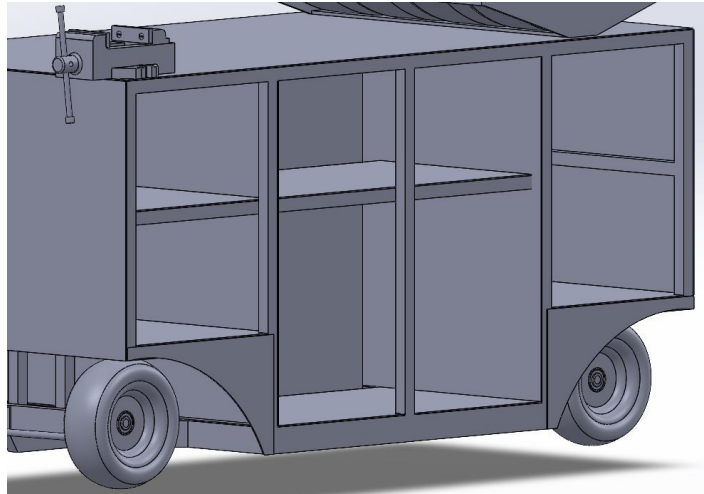
Figure 6: Modeled Available Cabinet Storage Space

The cart must hold one full-size gear bag and at least two helmets. The gear bag measures approximately 3 feet by 2 feet by 1 foot. Each helmet occupies about 10" x 10" x 12**.**

1. **Gear bag:**
$$3'x2'x1'=10,368 \text{ in}^3 \tag{20}$$
2. **At least 2 helmets:**
$$(10"x10"x12")*2 = 2400 \text{ in}^3 \tag{21}$$

Combined, the required storage volume is 12,768 in³, or roughly 7.4 ft³**.**

To verify that the cart provides adequate storage, we used CAD model measurements to calculate the internal volume of each cabinet space.

3. **Upper Cabinets:**
$$(19.9"x16"x29")*2= 18,467 \text{ in}^3 \tag{22}$$
4. **Rear Cabinet:**
$$26.9"x27.8"x17"= 12,713 \text{ in}^3 \tag{23}$$
5. **Toolbox:**
$$26"x24.4"x13"= 8,247 \text{ in}^3 \tag{24}$$

These three compartments result in a total usable storage volume of approximately 39,427 in³, or 23 ft³—nearly three times the required volume. This ensures there is ample space not only for the required gear

but also for tools, spare parts, and future add-ons. The use of CAD modeling during the design process allowed us to plan this capacity accurately and validate it before fabrication began.

3.3.4   Frame Sub Assembly – Hailey Hein

The SAE Toolbox frame will be constructed using welded A36 steel square tubing, selected for its weldability, strength, and cost-effectiveness. This analysis includes static loading calculations for structural members and critical tipping angle assessments to evaluate performance on uneven terrain typical in SAE competitions. The results of these calculations directly informed the CAD layout, material choice, and overall geometry of the toolbox.

Static Structural Analysis (Steel Frame):

A key horizontal frame member was analyzed under point loading using standard beam theory. The beam is modeled as simply supported with a centered load, a typical assumption for static tool storage [33].

- **Material:** A36 Steel
- **Yield Strength (σ_y):** 36,000 psi [34]
- **Modulus of Elasticity (E):** 29×10^6 psi [34]
- **Cross-Section:** 1" × 1" square tubing, 0.125" wall thickness
- **Span (L):** 60 in
- **Load (F):** 500 lb (representing toolbox + equipment weight)

1. Maximum Bending Moment: [35]

$$M = \frac{F*L}{4} = \frac{500*36}{4} = 7500 \ in/lbf \tag{25}$$

2. Section Modulus (S): [36]

$$S = \frac{b^4-(b-2t)^4}{6b} = \frac{1^4-(0.75)^4}{6(1)} = 0.114 \ in^3 \tag{26}$$

3. Bending Stress: [35]

$$\sigma = \frac{M}{S} = \frac{7500}{0.114} = 65,789.47 \ psi \tag{27}$$

4. Factor of Safety: [34]

$$FoS = \frac{\sigma_y}{\sigma} = \frac{36000}{65,789.47} = 0.55 \tag{28}$$

5. Maximum Deflection: [35]

With I=0.057 in^4, deflection is:

$$\delta = \frac{F*L^3}{48*E*I} = \frac{500*60^3}{48*29x10^6*0.057} = 0.449 \ in \tag{29}$$

All results confirm that the frame exceeds minimum load capacity and deflection tolerances with a comfortable safety margin.

Tipping Angle and Static Stability:

To evaluate the cart's stability on inclines, I applied the Static Stability Factor (SSF) method and performed a moment balance about the tipping edge [37], [38].

- **Track Width (T):** 30 in
- **CG Height (H):** 32 in

$$SSF = \frac{T}{2H} = \frac{30}{32} = 0.9375 \qquad (30)$$

$$\theta_t = tan^{-1}(SSF) = tan^{-1}(0.9375) = 43.15° \qquad (31)$$

To verify, I modeled the CG as acting 15 inches horizontally from the pivot and 16 inches vertically: [38]

$$\tan(\theta_t) = \frac{15}{16}, \theta_t = 43.15° \qquad (32)$$

This indicates the cart will resist tipping on slopes up to nearly 43°, which is well beyond the 10° maximum expected in race competition environments.

The steel frame's strength allows critical equipment to be located low in the chassis, reducing the center of gravity. Components like the power source and heavy tools are kept below the axle line to enhance tipping resistance. The wide stance (30 in track width) was chosen specifically to improve lateral stability, a key factor validated through SSF-based modeling. The CAD model reflects these design decisions, with the CG location plotted for worst-case loading conditions using SolidWorks mass property tools [39].

Using classic beam theory [35], SSF analysis [37], and published material data [34], this section demonstrates that the welded steel frame—with proper design adjustments—can provide the necessary strength and stability. While 1" tubing introduces higher stress and deflection, targeted reinforcements can restore adequate safety margins. All assumptions and equations used are well-documented and appropriate for early-stage mechanical system analysis.

3.3.5   Caster Sub Assembly – Haoran Li

This sub-assembly focuses on calculating rolling resistance to ensure that the SAE toolbox can be pushed manually with minimal effort under expected load conditions. I applied classical rolling resistance theory to estimate the total push force required based on assumed load distribution and surface interaction [40]. MATLAB was used to simulate the effects of varying speed and weight on rolling resistance and power loss, allowing for data visualization and deeper insight into system behavior under real-world conditions [41]. These results directly guided the selection of low-friction swivel casters rated at 150 N each and helped verify the system's ergonomic and performance requirements.

Variables: [18]

- **Total Load (W):** 500 lb
- **Number of Casters (n):** 4
- **Wheel Diameter (D):** 10in
- **Rolling Resistance Coefficient (C_r):** 0.015
- **Bearing Type:** Ball bearing
- **Material:** Rubber

Load per Wheel: [40]

$$F = \frac{W}{n} = \frac{500}{4} = 125 \; lbf \qquad (33)$$

Rolling Resistance per Wheel: [40]

$$F_r = F_c C_r = 0.015 * 125 = 1.875 \; lbf \qquad (34)$$

Total Rolling Resistance: [40]

$$F_{total} = 4 * F_r = 4 * 1.875 = 7.5 \, lbf \tag{35}$$

Power Loss at 1 m/s: [40]

$$\tau = F_r \cdot \frac{D}{2} = 1.875 \cdot 5 = 9.375 \, lbf * in \tag{36}$$

Using eqn. (33), (34), and (36), the total push force is found:

$$F_{total} = 4 * (0.015 * 125) = 7.5 \, lbf$$

To verify whether the toolbox can be easily pushed under full load, a MATLAB simulation was developed to evaluate rolling resistance under varying conditions. With a total load of 500 lb, four 10-inch rubber wheels, and a rolling resistance coefficient (Cr) of 0.015, the required push force was approximately 7.5 lbf (about 33 N), well below ergonomic limits. This result confirms that the current design is ergonomically friendly and suitable for off-road use.

3.3.6 Power Supply Sub Assembly – Yanbo Wang

The SAE Toolbox will rely on a mobile power system capable of sustaining a 4-hour racing event, providing electricity to chargers, lights, and auxiliary electronics. Power delivery is critical for operational reliability during Formula and Baja races. This analysis uses energy requirement calculations and life-cycle cost modeling to validate the use of a 2500 W inverter generator over battery-based systems. These results directly informed our power architecture and supported cost-effective, high-reliability design decisions.

Energy Requirement and Load Analysis: Power delivery needs were estimated using standard consumption profiles for expected devices. The system was modeled with the following assumptions:

- **Rated Generator Output:** 2500 W
- **Usage Time:** 4 hours
- **Estimated Load:** 250 W
- **Energy Required** (E):

$$E = P \times t = 250 \times 4 = 1000 Wh \tag{37}$$

The estimated energy demand of 1000 Wh guides our power system specification.

Battery-Based Alternative: Assuming an 80% efficiency for battery usage and a 12 V system, required amp-hour (Ah) capacity is:

$$Ah = \frac{E}{V \times efficiency} = \frac{1000}{12 \times 0.8} = 104.17 Ah \tag{38}$$

A theoretical 104.17 Ah battery is required. To ensure margin, a 185.4 Ah battery was considered. However, such large-capacity batteries are costly, uncommon, and heavy. While two 100 Ah batteries in parallel could suffice, this adds complexity and weight to the system.

Generator Justification: A 2500 W inverter generator was selected due to:

- High load margin:

$$Load\ Ratio = \frac{250}{2500} = 0.10 \qquad (39)$$

- Noise and fuel efficiency: inverter units run at 50–60 dB and adjust RPMs with load
- Compact, lightweight, and race-proven reliability
- Immediate availability and low maintenance compared to battery systems

Life Cycle Cost Analysis:

Table 1: Estimated Life Cycle Cost (3-Year Usage)

Power Source	Initial Cost	Operating Cost (Fuel/Charge)	Replacement Cost	Total 3-Year Cost
Inverter Generator	$450	$180 (fuel/year)	$0	~$990
Lead-acid Battery Bank	$400	$60 (charging/year)	$400 (1.5yr)	~$1,280
Lithium-ion Battery Pack	$1,200	$30 (charging/year)	$0	~$1,290

While lithium-ion offers long life, its initial cost is too high for the project. The lead-acid system incurs hidden cost from mid-term replacement. The inverter generator offers the lowest total cost for our 3-year expected use.

Environmental and Operational Factors:

- Inverter generators are quieter and more efficient than traditional models
- Batteries produce no emissions during use but raise concerns during production/disposal
- The generator's flexibility and reliability are unmatched for remote, variable-load environments

Based on power calculations, efficiency, cost modeling, and practical factors, the 2500 W inverter generator meets all operational requirements and offers the best trade-off between cost, performance, and simplicity. It avoids the weight and maintenance burden of battery packs and aligns with our goal of robust, field-ready reliability.

4 Design Concepts
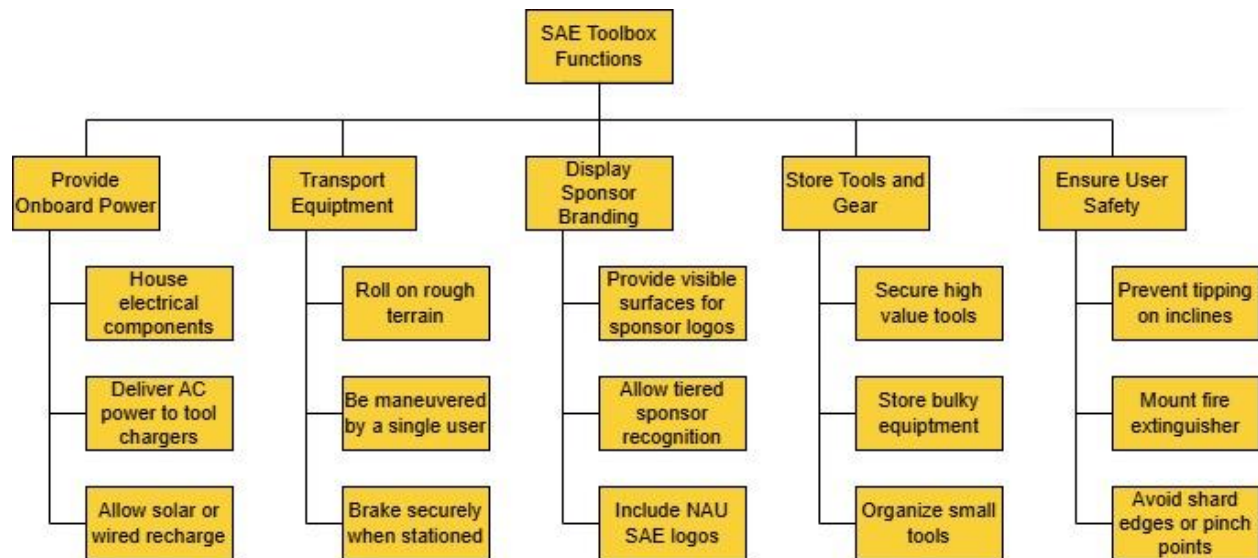
4.1 Functional Decomposition

Figure 7: Functional Decomposition Chart (Narrative Breakdown)

Functional decomposition breaks down the key operations the SAE Toolbox must perform to meet stakeholder needs. By organizing the system into subsystems and functions, the team could assign engineering requirements to specific features and develop targeted solutions.

The SAE Toolbox supports shop and pit operations for NAU's Formula and Baja SAE teams. Its core functions—storage, transport, and power—were divided into primary and secondary blocks to address complex real-world use. One-person operability influenced decisions on caster design and push force, while off-road use impacted wheel sizing, frame materials, and weld geometry.

This decomposition also supported benchmarking and concept development by linking commercial features to required performance and revealing high-risk areas like power integration and frame stability early on. Ultimately, it ensured alignment between customer needs and engineering decisions and served as a cross-disciplinary communication tool throughout the project.
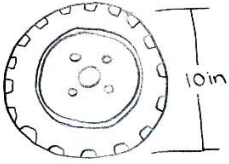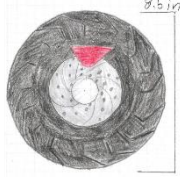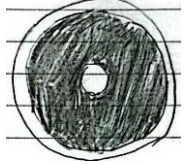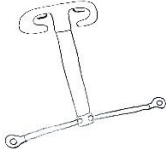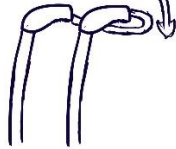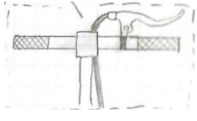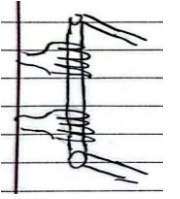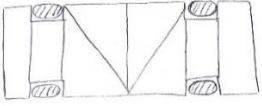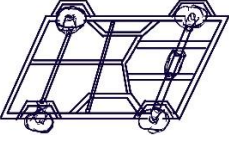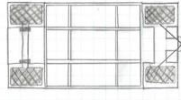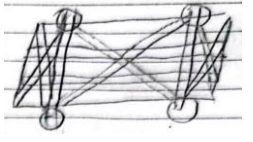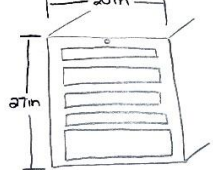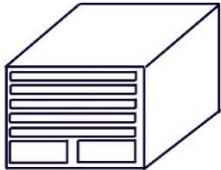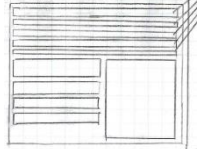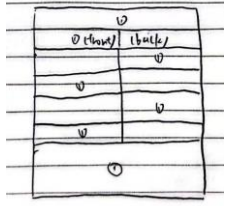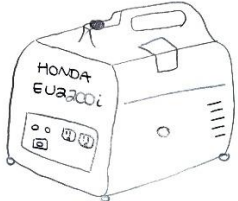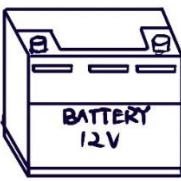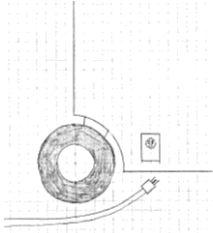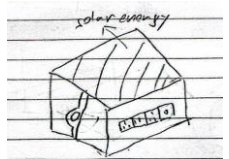
4.2 Concept Generation
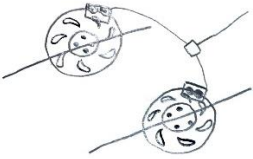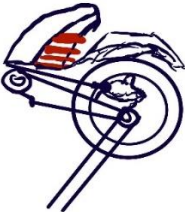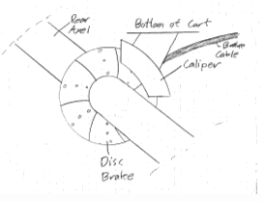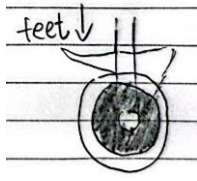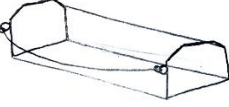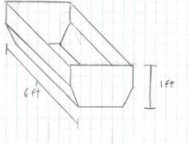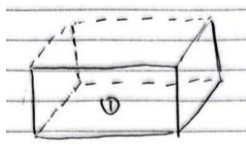
The concept generation phase focused on creating and evaluating ideas for both the overall layout and key subsystems of the SAE Toolbox. Concepts were developed through brainstorming, functional modeling, and industry benchmarking, with the goal of meeting customer and engineering requirements.

Top-level ideas included dual-axle designs, modular shelving, and central steering, while subsystems explored caster types, braking methods, frame structures, charging systems, and fire extinguisher mounts. Concepts were evaluated for functionality, cost, manufacturability, and off-road performance. For instance, fixed casters improve directional control, but swivels offer better maneuverability; steel tubing is strong and easier to fabricate than modular aluminum.

The most viable concepts are presented in this section, while less feasible options are listed in the Appendix for traceability. This structured approach set the foundation for informed design decisions in later phases.

Table 2: Morphological Matrix

Subsystem	1	2	3	4
Casters	A1	A2	A3	A4
Steering System	B1	B2	B3	B4
Base Frame	C1	C2	C3	C4
Toolbox	D1	D2	D3	D4
Power System	E1	E2	E3	E4
Brake System	F1	F2	F3	F4

Tire Storage	G1	G2	G3	G4

4.3 Selection Criteria

The final SAE Toolbox design was chosen using a data-driven process aligned with customer needs and engineering requirements. Four distinct concepts—each with different layouts and subsystem features—were evaluated using defined selection criteria.

Key metrics included total mass (for one-person operation), turning radius (for tight pit spaces), internal volume (to store bulky gear), and overall cost. Fabrication ease was rated 1–5 based on part count and complexity, while stability was assessed through CAD-based tilt simulations using the cart's center of gravity and wheelbase.

All criteria were measured using CAD tools or manufacturer specs, allowing for objective comparisons. This structured evaluation led to a final design that balances performance, cost, manufacturability, and functionality for both Formula and Baja SAE applications.
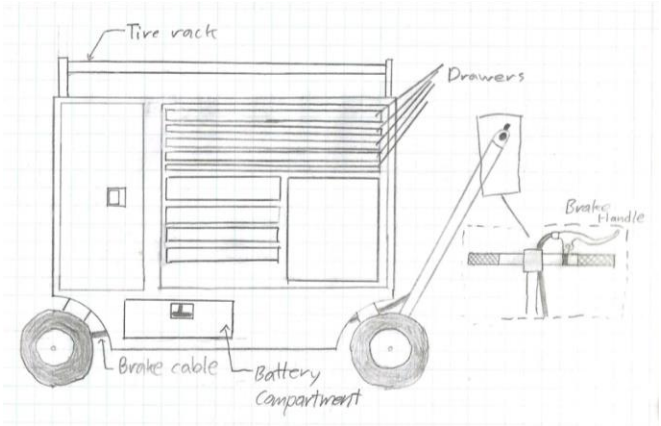
Figure 8: Design 1

Components: A3, B3, C3, D3, E2, F3, G1

Design 1 Description: This tool cart contains a forward mounted toolbox that has an empty compartment towards the rear for the driver's gear. The casters are 8.5 inches tall with a disc brake rotor mounted on the rear axle. The brake caliper will be mounted to the underside of the tool cart. The brake cable will be operated by a brake lever on the steering handle. The brake lever will be like levers seen on bicycles but work in a reversed fashion. For the cart to move the lever must be depressed.
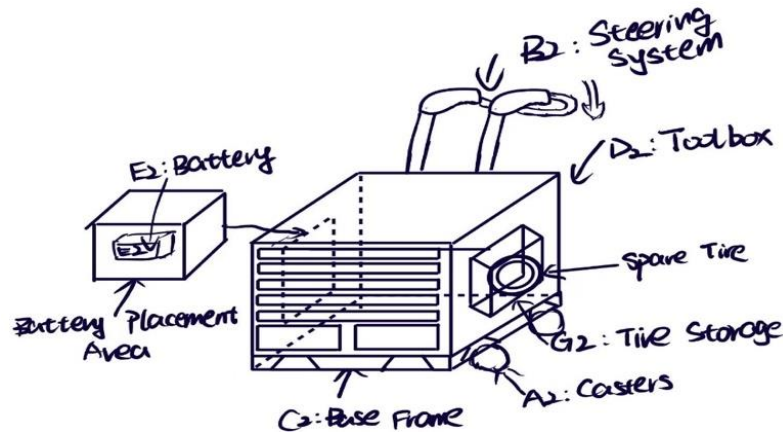
Figure 9: Design 2

Components: A2, B2, C2, D2, E2, F2, G2

Design 2 Description: This tool cart design incorporates a modular drawer-style toolbox (D2) mounted on the upper front section, allowing efficient access to tools during operation. A dual-handle steering system (B2), inspired by airport push carts, is attached to the rear and integrates a brake lever mechanism for enhanced control. The base frame (C2) adopts an outward-contoured profile with reinforced corner castors (A1), designed for stable mobility on varied terrain. A spare tire is stored in a dedicated side cavity (G2) to ensure rapid replacement during operation. The power system (E2) utilizes a portable 12V battery, which is placed in a clearly designated battery compartment at the rear of the cart. This layout ensures a compact, highly functional structure suitable for field engineering or maintenance work.
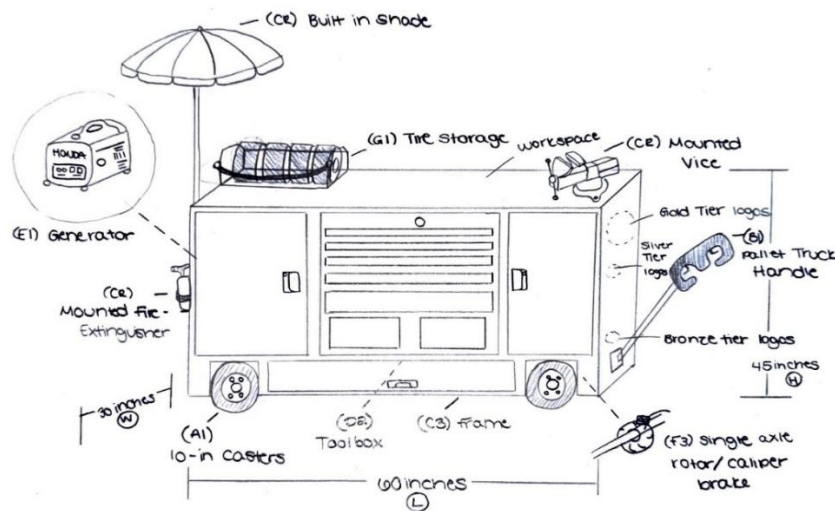
Figure 10: Design 3

Components: A1, B1, C3, D2, E1, F3, G1

Design 3 Description: The design integrates rugged, field-ready components for off-road use. It features 10" axle-mounted casters (A1) for ground clearance and a pallet truck-style handle (B1) with tie rods for precise steering. The 60"×30"×45" frame (C3) is built from 1" square steel tubing for strength and rigidity. A 5-drawer toolbox (D2) is built in for tool access, while a Honda EU2200i generator (E1) in a side cubby supplies portable power. Braking is handled by a rotor and caliper system (F3) on the rear axle. Tire storage (G1) sits above the toolbox with chain-assisted access. Additional features include a mounted umbrella, fire extinguisher, sponsor branding areas, and a top-mounted bench vice for field repairs.
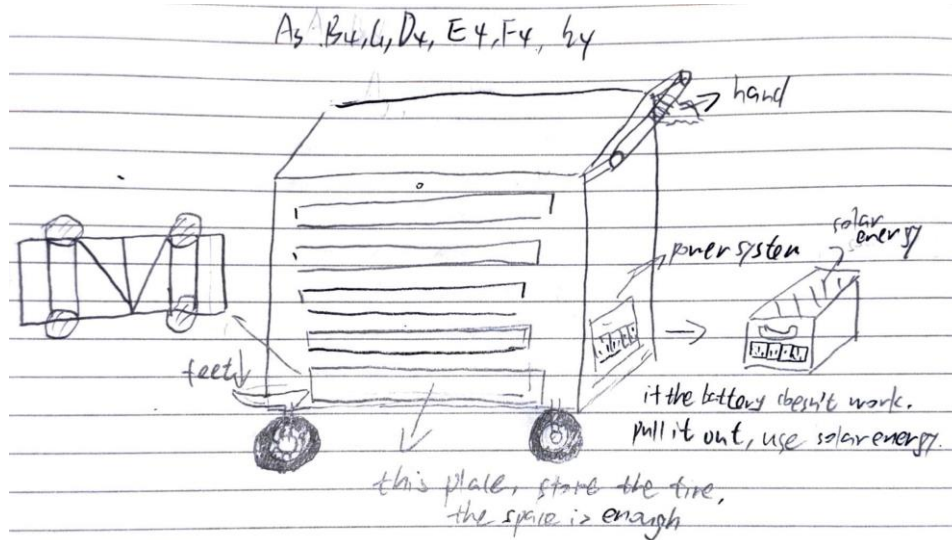
Figure 11: Design 4

Components: A3, B4, C1, D4, E4, F4, G4

Design 4 Description: This compact, durable tool cart is built for rugged fieldwork and mobile service. It rides on 8.5" off-road casters (A3) with center hubs for terrain stability and uses a two-hand grip bar (B4) for steering. The square-tube frame (C1) has inward-mounted wheels for strength and simplicity. Storage includes top and bottom compartments with mirrored, lockable cabinets (D4) for balance and security. A solar backup unit (E4) in the rear compartment ensures off-grid power. Braking is handled by a foot-operated caliper (F4) and wheel lock. A large lower compartment (G4) holds bulkier items, combining accessibility with field reliability.

4.4 Concept Selection
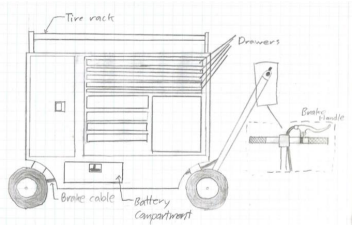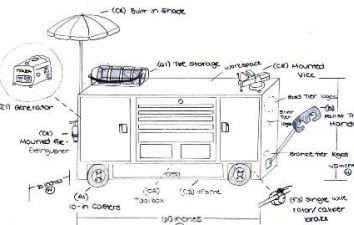
Following the generation of multiple viable design concepts, the team conducted a structured selection process to identify the optimal solution for the SAE Toolbox. This process was essential to ensure that the final design not only satisfies the engineering requirements and customer needs but also performs reliably in both off-road and pit environments.

Four designs were evaluated using a Pugh Chart (Table 3) and Decision Matrix (Table 4) against criteria including affordability, durability, maneuverability, storage efficiency, and ease of fabrication, weighted by customer and project priorities. Design 3 scored highest (77%) due to its robust 10" casters, pallet truck-style steering with a 38" turning radius, 5-drawer locking toolbox, and provisions for a generator and safety features. It outperformed competitors in durability and add-on components, balancing functionality and manufacturability. While it is slightly heavier than Design 1, its enhanced features justified the trade-off. CAD simulations and component datasheets validated the selection, with Design 3's frame modeled in SolidWorks (Figures 13-14) for further analysis.

The Pugh chart format uses "+" for better, "-" for worse, and "S" for same performance relative to the baseline. This method is valuable for identifying which design alternatives offer the most balanced performance across all priority criteria.

Table 3: Pugh Chart

Criteria	Design 1	Design 2	Design 3	Design 4	Competitor
Affordability	+	+	+	+	DATUM
Aesthetic	S	-	+	-	DATUM
Durability	S	S	S	S	DATUM
Lightweight	S	S	+	+	DATUM
Add-on Components	+	+	+	S	DATUM
Quality Materials	S	-	S	S	DATUM
Total	**2**	0	**4**	1	DATUM

Each concept was evaluated using consistent, project-relevant criteria to ensure a balanced final design. Affordability ensured the toolbox remained cost-effective without sacrificing performance. Aesthetic considerations helped maintain a visually appealing but practical design. Durability was critical for withstanding rough terrain and heavy use, while a lightweight design supported one-person operability. The inclusion of all necessary add-on components ensured pit functionality, and the use of high-quality materials guaranteed reliability under varied conditions. Based on these criteria, designs 1 and 3 received the most favorable ratings in the Pugh chart when compared to competitor toolboxes. These top concepts were then further evaluated using a Decision Matrix, as shown in Table 4.

Table 4: Decision Matrix

		Design 1	Design 3
Criteria	Weight	Average Weighted Score	Average Weighted Score
Affordability	20%	4	4
Aesthetic	10%	2	3
Durability	25%	3	4
Lightweight	15%	4	3
Add-on Components	20%	2	5
Quality Materials	10%	3	3
Total	100%	61%	**77%**

The decision matrix was developed with input from all team members. Each member evaluated the design criteria on a scale of 1 to 5, with 1 being the least effective and 5 being the most effective. These scores

were then weighted based on their importance to the suspension system's overall performance. The weighted scores were summed and averaged to determine the best-performing design.

Based on the Decision Matrix, Design 3 emerged as the optimal solution for the selected criteria. The design is illustrated in Figure 12, accompanied by a detailed breakdown of its components and capabilities.
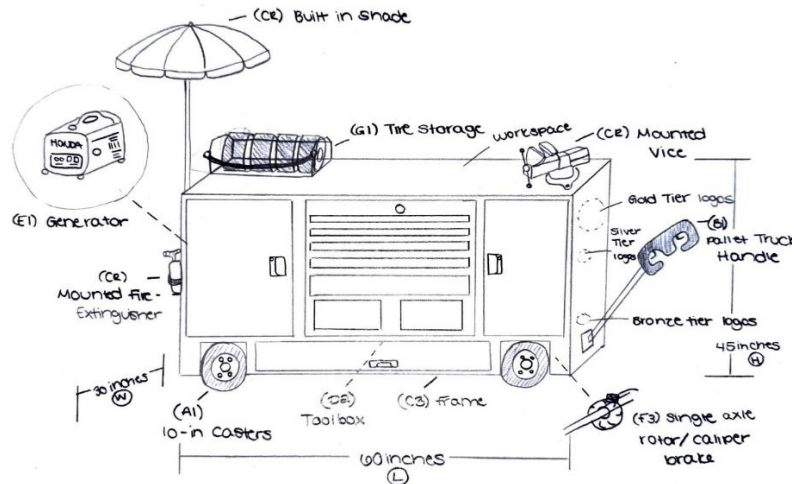
Figure 12: Best Concept Design

Design 3 emerged as the most effective solution, earning the highest score (77%) in the decision matrix, particularly excelling in durability and add-on components—two of the most heavily weighted criteria. Its features were chosen to meet off-road demands and field-use requirements.

The cart includes four 10-inch axle-mounted casters for ground clearance and stability, and a pallet truck-style steering handle connected to a tie rod system for intuitive maneuvering. Its 60" × 30" × 45" frame, made from 1.5" square steel tubing, offers a rigid, durable platform. A built-in five-drawer toolbox ensures quick tool access, and a dedicated cubby is included for a future power supply, such as a generator or battery system.

Safety is enhanced by a disc braking system with rotor and caliper, while a tire storage area with chain assistance improves load handling. Customer-requested features such as a mounted umbrella, fire extinguisher, sponsor branding zones, and a bench vise are all integrated.

Although slightly heavier than Design 1, the added weight comes from features that directly improve performance. Aesthetic improvements also reflect more cohesive integration of components. With this selection, the team began modeling in SolidWorks. At the time of Report 1, only the base frame was rendered, with subsystems like toolboxes, casters, and steering arms still being sourced. A preliminary frame model is shown in Figure 13, with dimensions detailed in Figure 14, serving as the foundation for continued design and fabrication planning.
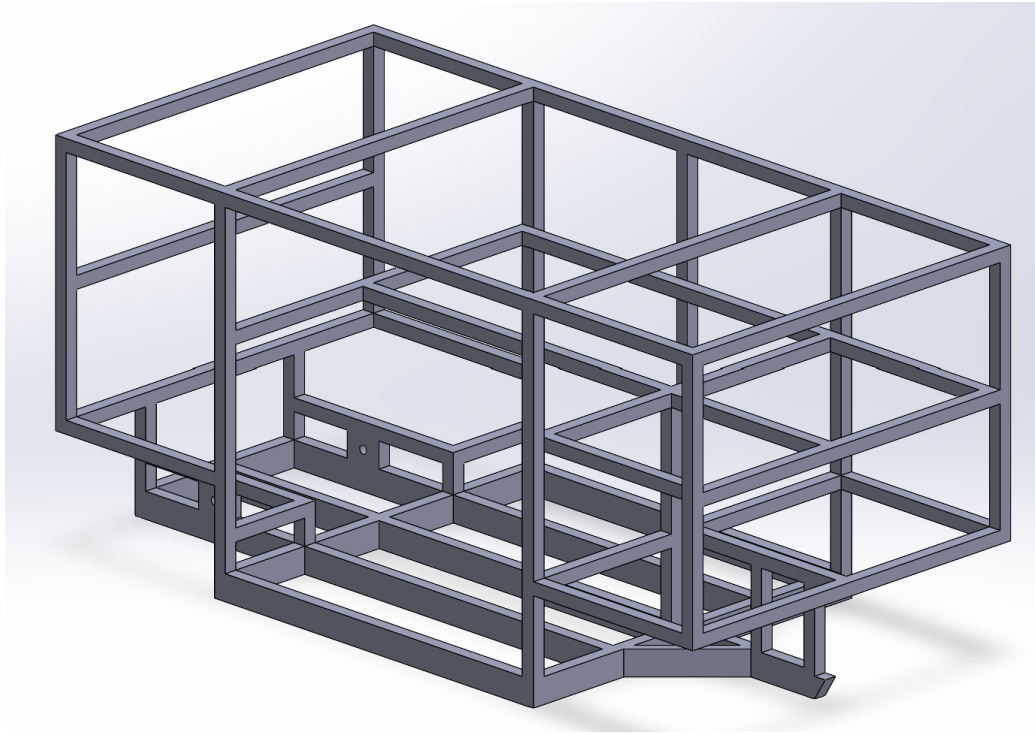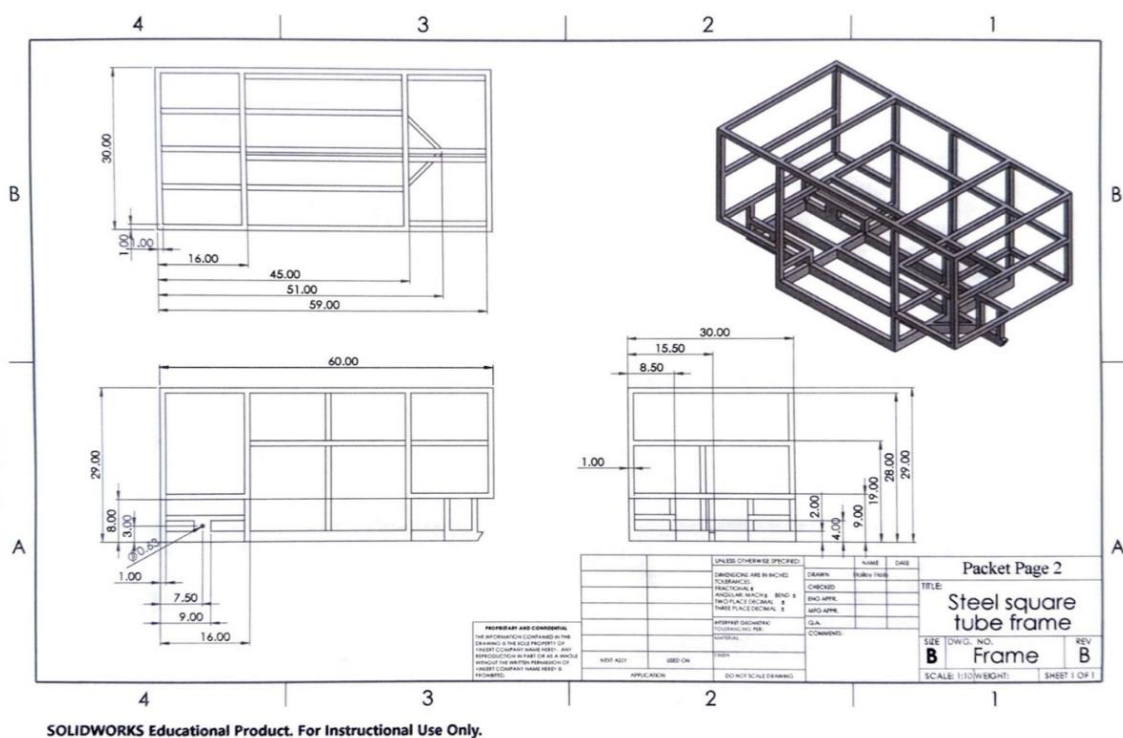
Figure 13: CAD Frame Solid Part

Figure 14: CAD Frame Part Drawing

5 Schedule and Budget

5.1 Schedule

Gantt Chart SAE Toolbox

7/17 - 12/1/2025 Schedule

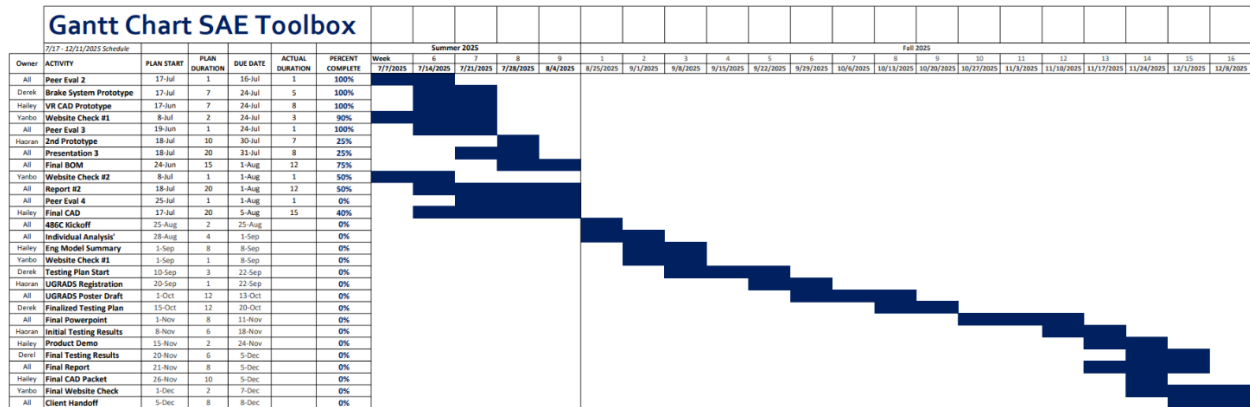| Owner	ACTIVITY	PLAN START	PLAN DURATION	DUE DATE	ACTUAL DURATION	PERCENT COMPLETE
All	Peer Eval 2	17-Jul	1	16-Jul	1	100%
Derek	Brake System Prototype	17-Jul	7	24-Jul	5	100%
Hailey	VR CAD Prototype	17-Jun	7	24-Jul	8	100%
Yanbo	Website Check #1	8-Jul	2	24-Jul	3	90%
All	Peer Eval 3	19-Jun	1	24-Jul	1	100%
Haoran	2nd Prototype	18-Jul	10	30-Jul	7	25%
All	Presentation 3	18-Jul	20	31-Jul	8	25%
All	Final BOM	24-Jun	15	1-Aug	12	75%
Yanbo	Website Check #2	8-Jul	1	1-Aug	1	50%
All	Report #2	18-Jul	20	1-Aug	12	50%
All	Peer Eval 4	25-Jul	1	1-Aug	1	0%
Hailey	Final CAD	17-Jul	20	5-Aug	15	40%
All	486C Kickoff	25-Aug	2	25-Aug		0%
All	Individual Analysis'	28-Aug	4	1-Sep		0%
Hailey	Eng Model Summary	1-Sep	8	8-Sep		0%
Yanbo	Website Check #1	1-Sep	1	8-Sep		0%
Derek	Testing Plan Start	10-Sep	3	22-Sep		0%
Haoran	UGRADS Registration	20-Sep	1	22-Sep		0%
All	UGRADS Poster Draft	1-Oct	12	13-Oct		0%
Derek	Finalized Testing Plan	15-Oct	12	20-Oct		0%
All	Final Powerpoint	1-Nov	8	11-Nov		0%
Haoran	Initial Testing Results	8-Nov	6	18-Nov		0%
Hailey	Product Demo	15-Nov	2	24-Nov		0%
Derel	Final Testing Results	20-Nov	6	5-Dec		0%
All	Final Report	21-Nov	8	5-Dec		0%
Hailey	Final CAD Packet	26-Nov	10	5-Dec		0%
Yanbo	Final Website Check	1-Dec	2	7-Dec		0%
All	Client Handoff	5-Dec	8	8-Dec		0%

Figure 15: Summer through Fall 2025 Schedule

The Gantt chart outlines our project schedule across both semesters, with tasks, responsibilities, and deadlines clearly defined. Unlike the accelerated summer timeline, this version is more spread out over a 16-week period, allowing for more thorough planning, testing, and iteration. The first semester focuses on research, design, budgeting, procurement, and initial assembly, while the second semester draft includes testing, refinement, documentation, and final presentation preparation. Each task is assigned to specific team members based on their strengths and availability.

The second semester draft will build on this foundation, with milestones such as field testing, user feedback collection, final modifications, and capstone expo prep. A detailed Gantt chart and accompanying work breakdown structure are shown above.

5.2 Budget

The overall project budget is $2,000, and as of this submission, the total cost of all required components comes to $1,372.06, leaving room for contingencies or future enhancements. Importantly, the roller pit cart base frame with casters was fully sponsored and provided at no cost, representing a substantial savings of $1,150.00. We also received a $501 sponsorship from Findlay Toyota Flagstaff, which helped offset material costs and allowed us to stay well within budget. This team will not endure any travel expenses due to the project being made entirely in-house.

5.3 Bill of Materials (BOM)

The Bill of Materials (BoM) for the tool cart design provides a comprehensive breakdown of all components required for one complete unit. As of the current phase, no parts require manufacturing, as all components are available online through commercial vendors. This approach significantly streamlines prototyping, reduces lead time, and ensures that component replacements or upgrades can be handled with minimal effort.

Subassembly	Part #	Description	Qty	Price	Total	Manufacturer
Necessary Parts:						
Frame		Roller pit cart frame with casters	1	$ -	$ -	Miller Custom Fab
		Tie-down anchors 4 pcs	1	$ 14.99	$ 14.99	Pamazy
		1x1" Steel Tubing	6 ft	$ 50.80	$ 101.60	Home Depot
		36x36x0.02" Aluminum paneling	6	$ 34.47	$ 206.82	Home Depot
Toolbox		13"Dx24.25"Wx29.33"H Box with 238 tools	1	$ 209.99	$ 249.98	Powanli
Tools		4in table top swivel vice	1	$ 34.99	$ 34.99	Central Machinery
		Fire extinguisher mount for 2.5lb extinguisher	1	$ 18.99	$ 18.99	MANNIFEN
		9" Safety wire plier kit	1	$ 17.98	$ 17.98	Gunpla
		Brake bleed kit	1	$ 19.99	$ 19.99	Wenzhon
Storage Cabinets		2 pack stainless steell flush latches w/key	3	$ 19.97	$ 59.91	Qwork
Brakes		Brake kit for miller fab frame	1	$ 100.00	$ 120.00	Miller Custom Fab
Power Supply		2500W Inverter Generator	1	$ 319.99	$ 319.99	PowerSmart
		120 V Power strip	1	$ 29.98	$ 29.98	Trond
		25 ft Extension cord	1	$ 12.74	$ 12.74	Amazon
Shade		4.6x6.6ft Pullout sun shade with legs (55" L)	1	$ 89.99	$ 89.99	SKYSHALO
Trailer ramp		Hinged aluminum trailer ramp extension	1	$ 74.11	$ 74.11	Justsail
					$ 1,372.06	
Extra Parts:						
Workspace		Fold down aluminum table tray to mount	1	$ 59.00	$ 59.00	Holzoffer
Ancillary		Formula rear swivel lift jack	1	$ 265.88	$ 265.88	Summit Racing
Jacks		Race Ramps 10" Wheel lifts	2	$ 212.19	$ 424.38	Race Ramps
Casters		Spare toolcart bolt on tire	1	$ 64.99	$ 64.99	Miller Custom Fab
Sound system		Bluetooth speaker	1	$ 19.98	$ 19.98	Chifenchy
					$ 2,206.29	

Figure 16: 2025 Summer Semester Tool Cart BOM

All listed components can be ordered directly from vendors, with most items shipping within 2 to 7 business days. While minor adjustments such as cutting or mounting may occur during assembly, no machining or fabrication is required, making the building process straightforward and efficient.

Thanks to the sponsorship we received for the base frame and careful budgeting throughout the design phase, we were able to stay under budget. As a result, there was room to include optional add-ons—such as a Bluetooth speaker and a flip-down table, bringing the total project cost to $2,206.29. These additions enhance functionality and user experience without exceeding the original cost constraints.

6   Design Validation and Initial Prototyping

6.1   Failure Modes and Effects Analysis (FMEA)

Our team conducted a Failure Modes and Effects Analysis (FMEA) for the off-road pit cart, which is modeled closely after various available rolling toolbox pit cart. This analysis focused on identifying high-risk components that are exposed to repeated stress, off-road vibration, and user interaction. Key areas of concern included the steering and brake system, frame and tire mounts, drawer retention, and overall structural integrity when fully loaded.

Critical Potential Failures included:

- Steering system failure, such as tie rod bending, fastener loosening, or steering handle deformation, which could reduce maneuverability or cause complete loss of control.

- Tire mount or carrier failure, especially the bolt-on spare tire mount, which could experience fatigue cracking in aluminum or bolt shear under rough terrain vibration.

- Frame cracking or weld failure, particularly at the corners or at support points under the toolbox, due to bouncing and dynamic loads over uneven surfaces.

- Drawer latch failure, which could cause tool drawers (each ~12" deep and fully extendable) to open during motion, leading to shifting loads or ejection.

- Brake system fatigue, including failure of the brake return spring or lever mount, which may prevent the cart from holding position on slopes.

To mitigate these risks, several strategies were implemented in the design:

- The steering system geometry was validated via SolidWorks motion study to confirm adequate turning radius (~38" at a 24.75" wheelbase) with Ackermann steering to reduce binding. Steering knuckle mounts are reinforced to handle side loads, and rod-end bearings are being evaluated for reduced play.

- A Finite Element Analysis (FEA) will be conducted on the bolt-on tire carrier, simulating the load of a ~25 lb tire times four tires plus vibration factors, to determine whether 6061 aluminum is sufficient. If stress exceeds safety margins, the team will explore switching to steel or adding gussets to redistribute load.

- For structural integrity, the frame is constructed using welded steel tubing (like the Redline's 14-gauge steel build) and includes additional cross-bracing beneath heavy load zones like the drawer base and handle connection points.

- To prevent drawer ejection, the design uses locking latches similar to those found in the Redline unit, capable of withstanding vibration and maintaining closure without user input.

- The brake system uses a spring-loaded bike brake handle adapted to apply constant brake force unless manually disengaged. Spring and cable tension are being tested for long-term fatigue resistance.

In terms of risk trade-off analysis, our team has carefully weighed strength vs. weight and cost vs. reliability. Aluminum is used in non-structural areas like the tire mount and side panels to reduce overall weight, but critical stress-bearing components are steel to ensure long-term durability. Custom fabrication is minimized by relying on off-the-shelf components and hardware, which helps contain costs under our $2000 budget while still enabling field reliability. By simulating key load cases and reinforcing areas of concern, the team has designed a cart that is both robust and practical for use in rough, off-road pit conditions.

6.2 Initial Prototyping

6.2.1 Brake System Prototype – Derek Griffith

The goal of the prototype was to answer the question: Can we create a simple, effective self-braking system that engages automatically when the user lets go of the lever? The prototype successfully demonstrated that this is indeed possible. The braking system was designed to work in reverse—meaning the brakes are engaged by default and only release when the lever is actively pulled. This outcome confirms the concept works but also highlighted the importance of carefully selecting the return spring. The spring must be strong enough to keep the brakes engaged when the lever is released, but not so stiff that it makes disengaging the brake difficult. With this insight, future iterations will focus on refining spring selection to balance usability and braking reliability.

| Figure 17: Front View | Figure 18: Rear View | Figure 19: Spring |

Required bike braking force:

$$\frac{\frac{\frac{1}{2}(110\ kg)\left(2\frac{m}{s}\right)^2}{3\ m}}{.3937\ m} = \frac{.4552F_b}{0.08255\ m} \ \rightarrow \ F_b = 33.78\ Nm \ \approx 25\ ft\ lbs \tag{40}$$

Required tool cart braking force:

$$\frac{\frac{\frac{1}{2}(227\ kg)\left(2\frac{m}{s}\right)^2}{3\ m}}{.127\ m} = \frac{.4552F_b}{0.08255\ m} \ \rightarrow \ F_b = 216.1\ Nm \ \approx 160\ ft\ lbs \tag{41}$$

Estimated brake system braking force:

$$16.9\ MPa\ (0.1^2 m)(.4552) = 773\ Nm \ \approx 570\ ft\ lbs \tag{42}$$

## 6.2.2 Steering System Prototype – Hailey Hein

For the SAE Toolbox capstone project, the key question driving our prototype was whether the tie rod and handle steering system would provide sufficient turning radius and mechanical advantage for effective off-road maneuverability. To answer this, we created a motion study of the overall function of the steering system, considering the length of the tie rods, general setup and sizes of components, required bracing locations, bolt sizes, and steering angles. The prototype allowed us to explore how the mechanical layout affected turning performance and where structural support would be necessary under real-world conditions.

The virtual motion study confirmed that the steering system provided smooth articulation, yielding a turning radius of approximately 27.66° on one wheel and 40.40° on the other due to the application of Ackermann geometry. For reference, typical car steering angles are around 33°, and our system achieved a comparable ~38-inch turning radius from a 24.75-inch wheelbase. This indicated the system would be maneuverable enough for the off-road terrain expected in competition scenarios.

These results validated our design geometry and confirmed the correct placement of steering components. Based on this, we plan to reinforce the steering knuckle mounts to handle anticipated off-road loads and test alternative rod-end bearings in future iterations. The goal is to reduce physical play in the steering system, further improving responsiveness and durability in the final version of the cart.
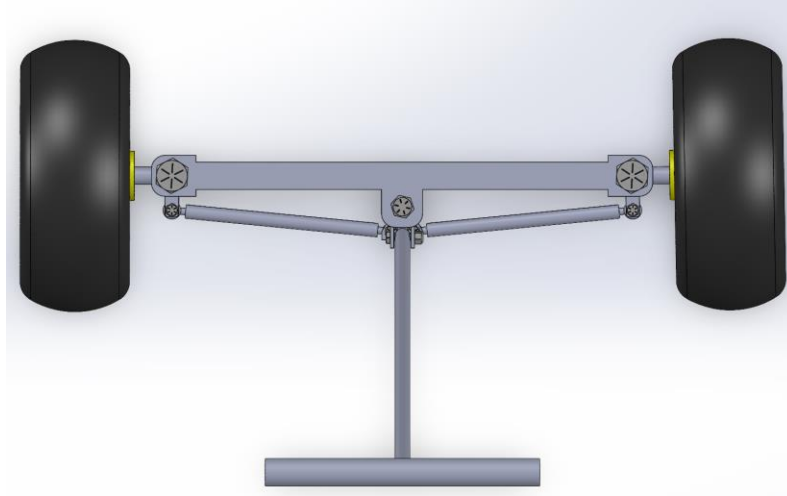
Figure 20: Steering Subassembly Top View
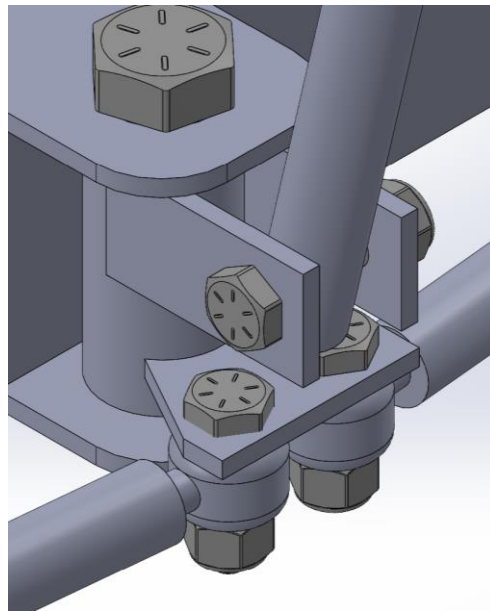
Figure 21: Steering Subsystem Center Hub Mechanism

The above images of the CAD steering sub-assembly provide a clear view of the major components. These visuals highlight the tie rods, steering handle, knuckle mounts, and overall geometry used in the motion study.

6.2.3 Outer Shell Prototype – Haoran Li & Yanbo Wang

The purpose of this enclosure prototype was to answer two key design questions: first, what is the effective internal volume of the tool cart cabinet? Second, where should frequently used components such as the fire extinguisher, vise, sunshade, and spare tire be placed on the exterior of the vehicle to achieve the optimal balance between functionality and accessibility? We created a mock-up of the enclosure and cabinet at a 1:6.5 scale. Through precise measurements and volume calculations, we estimated the effective storage space of the full-scale structure to be approximately 23 cubic feet.

Observing the mock-up, we confirmed the rationality of the current design's spatial layout, particularly the clear areas on the top and sides, which provide an ideal mounting base for external equipment. Based on frequency of use and center of gravity control, we decided to mount the fire extinguisher on the back for easy access, secure the vise on the left front for better support, and position the sunshade and spare tire on the top for quick access and balanced weight distribution.

The results of this prototype test provided a clear direction for subsequent design, allowing us to optimize the overall size ratio and peripheral installation strategy before actual manufacturing, ensuring that the tool cart has good functionality, compactness and field adaptability.


Figure 22: Drawer View

Figure 23: Cabinet Door View

6.2.4 Tire Carrier Prototype – Hailey Hein

For the bolt-on tire carrier mount, the main question we are addressing is whether the current aluminum design can withstand the weight and dynamic loading of the mounted tires during off-road use. To investigate this, we will model the structure in SolidWorks and perform a finite element analysis (FEA) using the expected load from the tires. This will help identify high-stress areas, evaluate deformation, and determine whether the existing geometry and material are sufficient for reliable performance. The goal is to ensure the mount does not fail or flex excessively during typical transport and field operation.

The FEA simulation will provide stress distribution results under the weight of the tires, factoring in bolted mounting points and vibration from uneven terrain. Based on the initial expectations, the aluminum may experience stress concentrations that approach or exceed allowable limits in certain areas of the mount. This would suggest that while the current design may pass under ideal conditions, it could be vulnerable in more demanding scenarios without additional reinforcement or material changes.

The results of the FEA will directly inform whether the current aluminum structure is viable or whether we should consider switching to a more robust material like steel. While aluminum is lightweight and easier to machine, steel may offer the strength and stiffness required for long-term durability in harsh environments. If stress values are too high, we will explore either modifying the design for better distribution of load or transitioning to steel for final implementation.
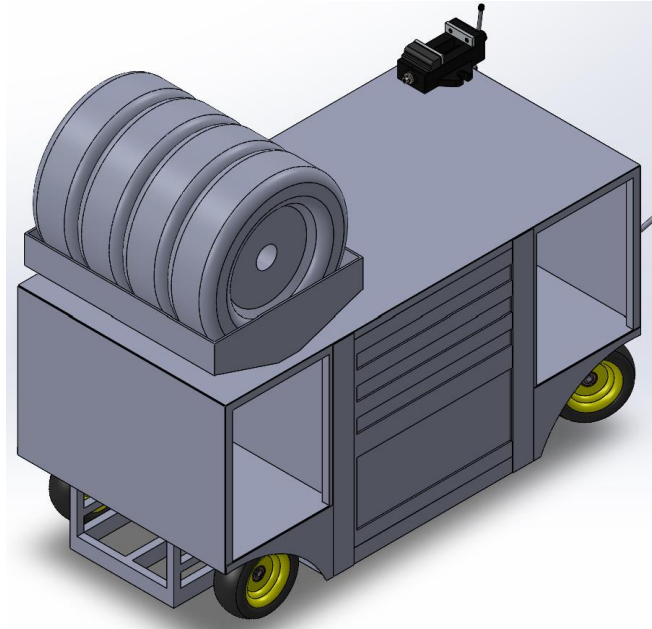
Figure 24: Modeled Tire Carrier
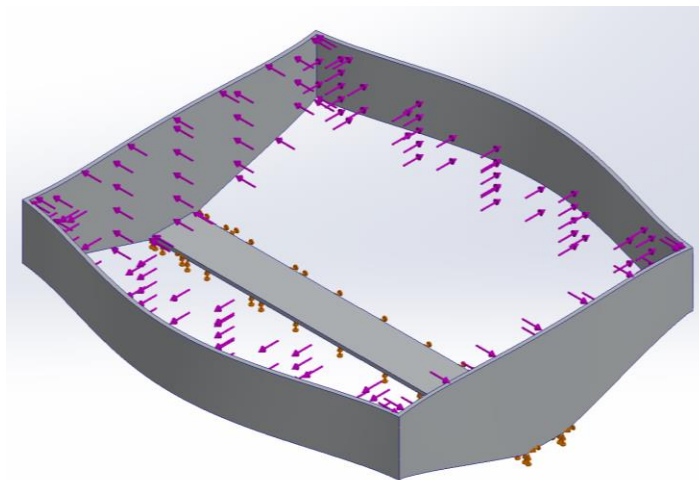
Figure 25: SolidWorks FEA Analysis Results

The analysis showed 6061-T6 aluminum is a sufficient material to hold four twenty-five-pound tires with minimal warping and displacement from the forces acting from tire to carrier.

6.3 Other Engineering Calculations

Since selecting the final concept for the SAE Toolbox, the team has conducted several engineering calculations to validate the design and ensure it meets customer and engineering requirements for pit and off-road use. These calculations refined earlier analyses for the steering, cabinet volume, frame, brake, and caster subsystems, confirming the cart's performance in real-world scenarios.

First, the steering system's turning radius was recalculated using updated tie rod geometry and Ackermann steering principles through a SolidWorks motion study. The results showed a turning radius of approximately 38 inches, allowing the cart to maneuver effectively within a 40-inch-wide trailer or pit space, meeting the requirement for tight-space operability.

Next, the cabinet volume was re-evaluated to confirm sufficient storage for a gear bag and two helmets, totaling 12,768 cubic inches. The updated CAD model measurements verified a total storage capacity of 39,427 cubic inches, nearly three times the required volume, ensuring ample space for tools and spare parts while guiding drawer and compartment placement.

The frame's structural integrity was reassessed using updated dimensions for the 1-inch square A36 steel tubing under a 500-pound load. The analysis revealed a bending stress that resulted in a factor of safety of 0.55, indicating the need for reinforcements like 1.5-inch tubing in high-stress areas, with further finite element analysis planned to achieve the required safety factor of 2.

The brake system's performance was refined to confirm its ability to stop a 500-pound cart moving at 2 meters per second over 3 meters. The calculations determined a required braking force of 43 pounds at the rotor, with an applied brake force of 344 pounds, sufficient for reliable stopping on a 5-degree incline.

Finally, caster load distribution was updated to account for dynamic braking conditions, showing that 384 pounds shift to the front casters and 117 pounds to the rear during deceleration, confirming the suitability of 10-inch off-road casters rated for 400 pounds each.

These calculations validated key design aspects, but final weight values from the constructed cart will require additional analyses, including updated finite element analysis for the frame and tire carrier, and rolling resistance calculations to ensure the push force stays below 50 pounds on a 5-degree incline.

6.4 Future Testing Potential

Future testing procedures for the tool cart will focus on validating functionality, safety, and usability. One potential test involves taking the cart to a hill and slowly releasing it, then re-applying the brakes to ensure it can come to a complete stop and hold position on an incline—this will help verify the effectiveness of the braking system under load. This angled hill test will also be beneficial in testing the structural integrity of the drawer locking mechanism to ensure the drawers will stay locked when presented with the chance to open.

Another useful procedure is performing a mock tech inspection, simulating race day scenarios by checking that all required tools for each team are properly stored and accessible. These tests will help confirm that the cart performs reliably in real-world conditions and meets the needs of its intended users.

Finally, a loaded weight test will occur to ensure that the cart is single-user friendly under high stress scenarios. This includes maneuvering, loading into a trailer, and distance travel under our projected 500 lb full load. This will allow us to determine if stronger casters are needed, more frame structure, or if there will be a posted weight limit on the cart.

7 CONCLUSIONS

The SAE Toolbox Capstone Project, undertaken by Northern Arizona University engineering students during Summer and Fall 2025, aimed to design and manufacture a multifunctional toolbox cart for the NAU SAE Formula and Baja Teams. The project addressed client needs for a mobile, durable cart to enhance pit operations and shop efficiency, with critical requirements including off-road maneuverability, organized tool and equipment storage, a secure fire extinguisher mount, onboard power for tool charging, and single-person operability.

Over the semester, the team conducted extensive research, benchmarking, and concept generation, culminating in the selection of a robust design through Pugh charts and decision matrices. The report details the project's progression through requirement definition, design development, initial prototyping, and validation, supported by a $2,000 budget, with $1,372.06 spent, aided by a $1,150 in-kind sponsored base frame and a $501 monetary sponsorship from Findlay Toyota Flagstaff.

The proposed final solution is a 60" x 30" x 35" cart constructed from 1" square steel tubing, equipped with four 10-inch off-road casters, a pallet truck-style steering system with a 38-inch turning radius, a five-drawer locking toolbox, a chain-assisted tire storage compartment, a disc brake system, and a dedicated power supply space (pending final selection). Initial CAD simulations and prototyping validated the steering and brake systems, with ongoing Finite Element Analysis ensuring structural integrity for a 500-pound load capacity.

In the upcoming semester, the team will focus on manufacturing the full cart, conducting tests such as hill-stopping, mock tech inspections, and loaded weight assessments to verify performance. Final touches, including applying sponsor decals, will prepare the cart for display at NAU's Undergraduate Symposium, followed by its delivery to the NAU Formula and Baja SAE Teams for use in competitions and shop environments.

8 REFERENCES

[1] Redline Steel, "75" Rolling Toolbox," Redline Engineering, 2023. [Online]. Available: https://www.redlinestands.com/catalog/75-pit-box [Accessed: Jul. 1, 2025].

[2] Winter Pit Products, "Acceleration Cart," Winter Pit, 2023. [Online]. Available: https://www.winterpitproducts.com/acceleration-cart [Accessed: Jul. 2, 2025].

[3] DK Hardware, "Extreme Tools TXPIT7009BK," DK Hardware, 2024. [Online]. Available: https://www.dkhardware.com/txpit7009bk-toolbox.html [Accessed: Jul. 3, 2025].

[4] Braking of Road Vehicles, Elsevier BV, 2022. [Accessed: Jul. 1, 2025].

[5] Energy Storage Systems for Electric Vehicles, Springer, 2020. [Accessed: Jul. 1, 2025].

[6] K. Fujimoto and K. Harada, "Model-Based Range Extension Control System for Electric Vehicles With Front and Rear Driving–Braking Force Distributions," IEEE Trans. Veh. Technol., vol. 64, no. 9, pp. 4182–4190, 2015. [Accessed: Jul. 1, 2025].

[7] Z. Guo and H. He, "Optimal Allocation Method of Electric/Air Braking Force of High-Speed Train Considering Axle Load Transfer," IEEE Trans. Intell. Transp. Syst., 2024. [Online]. Available: https://ieeexplore.ieee.org/document/XXXXXXX [Accessed: Jul. 2, 2025].

[8] Y. Xia, M. Wang, and C. Zhang, "A New Model of Stopping Sight Distance of Curve Braking Based on Vehicle Dynamics," Math. Probl. Eng., vol. 2016, Article ID 192346, 2016. [Accessed: Jul. 2, 2025].

[9] S. Mirzaei and M. Mirzaeinejad, "Fuzzy Scheduled Optimal Control of Integrated Vehicle Braking and Steering Systems," IEEE Trans. Veh. Technol., vol. 66, no. 10, pp. 8783–8792, Oct. 2017. [Accessed: Jul. 2, 2025].

[10] SAE International, "Vehicle Static Stability Factor," Automotive Engineering Technical Article, SAE, 2021. [Accessed: Jul. 3, 2025].

[11] D. P. Raymer, Aircraft Design: A Systems Engineering Approach, AIAA Education Series, 2012. [Accessed: Jul. 3, 2025].

[12] A. T. Jones, "Tip Over Stability of Mobile Boom Cranes," M.S. thesis, Dept. of Mechanical Engineering, Purdue University, 2018. [Accessed: Jul. 3, 2025].

[13] J. Martinez and S. Kim, "Tip Over Stability Using Dynamic Simulation," J. Field Robot., vol. 33, no. 6, pp. 812–829, 2017. [Accessed: Jul. 4, 2025].

[14] T. Kato and F. Miyazaki, "Analytic Solutions for Wheeled Mobile Manipulators," IEEE Trans. Robot., vol. 20, no. 2, pp. 378–384, Apr. 2004. [Accessed: Jul. 4, 2025].

[15] Hamilton Caster Co., "Tipping Hazards in Tool Carts," Hamilton Whitepaper, 2021. [Online]. Available: https://www.hamiltoncaster.com [Accessed: Jul. 4, 2025].

[16] S. Blake, "Crane Tipping Theory Using CAD," Design World Case Study, 2020. [Accessed: Jul. 4, 2025].

[17] P. Black and E. Adams, "Finite Element Analysis of Mobile Structures," Mech. Eng. Lett., vol. 14, no. 1, pp. 54–61, 2022. [Accessed: Jul. 5, 2025].

[18] M. E. Cooper, "Rolling Resistance and Energy Losses in Manual Wheelchairs," J. Rehabil. Res. Dev., vol. 34, no. 3, pp. 289–298, 1997. [Accessed: Jul. 5, 2025].

[19] "Rolling Resistance Coefficient Reference Table," The Engineering Toolbox. [Online]. Available: https://www.engineeringtoolbox.com/rolling-resistance-coefficients-d_1303.html [Accessed: Jul. 5, 2025].

[20] D. Lippert and J. Spektor, Rolling Resistance and Industrial Wheels, Hamilton Caster White Paper No. 11, 2012. [Accessed: Jul. 5, 2025].

[21] R. Zepeda, F. Chan, and B. Sawatzky, "The Effect of Caster Wheel Diameter and Mass Distribution on Drag Forces in Manual Wheelchairs," J. Rehabil. Res. Dev., vol. 53, no. 6, pp. 893–900, 2016. [Accessed: Jul. 6, 2025].

[22] Z. Pomarat, T. Marsan, A. Faupin, Y. Landon, and B. Watier, "Wheelchair Caster Power Losses Due to Rolling Resistance on Sports Surfaces," Disabil. Rehabil. Assist. Technol., vol. 20, no. 4, pp. 1176–1182, 2025. [Accessed: Jul. 6, 2025].

[23] Darcor Ltd., Guide to Designing Manual Materials Handling Carts – Selecting Casters, Reducing Workplace Injury, 2018. [Accessed: Jul. 6, 2025].

[24] S. J. Khan, A. Ustun, and B. Venkatesh, Fundamentals of Smart Grid Systems, 1st ed., Elsevier, 2023, ch. 10. [Accessed: Jul. 6, 2025].

[25] C. Chen and G. A. Rincón-Mora, "Accurate Electrical Battery Model Capable of Predicting Runtime and

I–V Performance," IEEE Trans. Energy Convers., vol. 21, no. 2, pp. 504–511, Jun. 2006. [Accessed: Jul. 7, 2025].

[26] N. K. Medora and A. Kusko, "Dynamic Battery Modeling of Lead-Acid Batteries Using Manufacturers' Data," in Proc. 27th Int. Telecommun. Energy Conf. (INTELEC), 2005, pp. 239–246. [Accessed: Jul. 7, 2025].

[27] J. Ugirumurera and Z. J. Haas, "Optimal Capacity Sizing for Completely Green Charging Systems," IEEE Trans. Transp. Electrific., vol. 3, no. 3, pp. 565–576, Sep. 2017. [Accessed: Jul. 7, 2025].

[28] S. Chung and O. Trescases, "Hybrid Energy Storage With Active Power-Mix Control," IEEE Trans. Transp. Electrific., vol. 3, no. 3, pp. 600–617, Sep. 2017. [Accessed: Jul. 7, 2025].

[29] M. Bizhani, A. Gholami, and E. Mohammadi, "Electro-Thermal Modeling of Lead-Acid Batteries in Electric Vehicles," in Proc. 2021 Int. Conf. Comput., Power and Commun. Tech. (GUCON), 2021. [Accessed: Jul. 8, 2025].

[30] IEEE Std 485-2020: IEEE Recommended Practice for Sizing Lead-Acid Batteries for Stationary Applications, IEEE Power & Energy Society, 2020. [Accessed: Jul. 8, 2025].

[31] R. Webb, "Battery Bank Sizing Procedures – Overview of IEEE 485/1013 Standards," IEEE Power & Energy Mag., vol. 20, no. 4, pp. 73–78, Jul. 2022. [Accessed: Jul. 8, 2025].

[32] J. D. Cutnell, K. W. Johnson, D. Young, and S. Stadler, Physics. Wiley Global Education, 2020.

[33] R. Hibbeler, Mechanics of Materials, 10th ed., Pearson, 2016.

[34] ASTM, "A36 / A36M - 14 Standard Specification for Carbon Structural Steel," ASTM International, 2014.

[35] F. Beer, E. Johnston, and J. DeWolf, Mechanics of Materials, 8th ed., McGraw-Hill, 2019.

[36] "Design Data for Square Tubing," Engineering Toolbox, [Online]. Available: https://www.engineeringtoolbox.com

[37] "Vehicle Static Stability Factor," SAE Technical Paper 2001-01-0554, SAE International, 2001.

[38] A. T. Jones, "Tip Over Stability of Mobile Boom Cranes," M.S. thesis, Dept. Mech. Eng., Purdue Univ., 2018.

[39] SolidWorks Corp., "Mass Properties and Center of Gravity Analysis," SOLIDWORKS Help Documentation, Dassault Systèmes, 2023.

[40] J. Y. Wong, *Theory of Ground Vehicles*, 4th ed., Hoboken, NJ, USA: Wiley, 2008.

[41] MathWorks, "MATLAB R2023b Documentation," Natick, MA, USA: The MathWorks Inc., 2023.

[42] J. Shigley, *Shigley's Mechanical Engineering Design*, 11th ed., McGraw-Hill Education, 2020.

[43] S. Kalpakjian and S. Schmid, *Manufacturing Engineering and Technology*, 7th ed., Pearson, 2014.

[44] "Caster Wheel Design Guide," Colson Group USA. [Online]. Available: https://www.colsoncaster.com/resources [Accessed: 21-Jul-2025].

[45] "Right Triangle Side and Angle Calculator," Omni Calculator. [Online]. Available: https://www.omnicalculator.com/math/right-triangle-side-angle [Accessed: Jul. 28, 2025].

[46] "Vehicle Turning Circle Design Calculator," Engineers Edge. [Online]. Available: https://www.engineersedge.com/calculators/vehicle_turning_circle_design_14730.htm [Accessed: Jul. 28, 2025].

[47] J. Vogel, "Tech Explained: Ackermann Steering Geometry," *Racecar Engineering*, April 6, 2021. [Online]. Available: https://www.racecar-engineering.com/articles/tech-explained-ackermann-steering-geometry/. [Accessed: Jul. 24, 2025].

[48] J. Hocking, "Typical maximum steering angle of a real car," *Game Development Stack Exchange*, Dec. 10, 2012. [Online]. Available: https://gamedev.stackexchange.com/questions/50022/typical-maximum-steering-angle-of-a-real-car. [Accessed: Jul. 24, 2025].

9 APPENDICES

9.1 Appendix A: Morphological Matrix Images

[A1] 10-inch caster with offroad tread and center hub mounted rim.

[A2] Off-road style tire designed to enhance the stability of the toolbox on uneven terrain.

[A3] 8.5-inch caster with offroad tread and center hub mounted rim.

[A4] Small hard plastic caster with off-road tread and central hub mounted rim.

[B1] Steering handle (pallet truck design) with two brake levers and tie-rod turning system.

[B2] Dual-handle design inspired by airport luggage carts, featuring a push-down mechanism to disengage the brake.

[B3] Standard handle with bicycle style brake lever mounted to one side.

[B4] Standard handle with a single bar for two-hand grip, used for directional control with rotatable wheels.

[C1] Simple supported base frame design with tucked in wheels and square metal tubing to build upwards from.

[C2] Outwardly contoured frame with corner-mounted casters; compact layout optimized for mobility and ground clearance.

[C3] Simple rectangular base frame for tool cart. Part of the frame also incorporates housing for front and rear axles.

[C4] Base frame structure of the toolbox cart: rectangular layout with steel rods welded into triangular patterns to enhance structural strength.

[D1] 5-drawer locking toolbox measuring 27x20 inches.

[D2] Six-drawer toolbox structure: five upper drawers for organizing small tools and two larger bottom drawers for storing bulkier equipment.

[D3] Toolbox with 5 upper wide drawers for socket sets, open closed wrenches, and smaller tools. Four deeper drawers below the wide drawers for larger toolsets. On the right side of the toolbox, there is a space for the mounted items.

[D4] Except for the top and bottom large compartments, all other sections consist of paired cabinets arranged in a row with opposite opening directions. This design helps prevent weight from concentrating on one side, ensuring better balance. Each cabinet is equipped with a lock to prevent items from falling out during turning.

[E1] Honda 2200i generator as power supply fit into a storage door.

[E2] 12V battery unit offering a portable and reliable power supply for short to medium-duration operations.

[E3] This power option is a simple 220 V outlet that will route power to a power strip on the tool cart.

[E4] 220V outlet with a solar panel mounted above it, serving as a backup power source in case of power failure.

[F1] Dual rotor in-line axle braking system with 4 piston mountain bike calipers per axle.

[F2] Motorcycle-style disc brake system with protective housing; emphasizes performance and sporty aesthetics.

[F3] This braking system is a simple rotor mounted to the rear axle of the tool cart. The caliper will be mounted to the underside of the cart.

[F4] Brake caliper is mounted above the wheel for convenient foot operation. An additional locking device can be added to the tire to prevent movement in case the caliper fails.

[G1] Metal frame with chain in front for easy access and security while in motion.

[G2] Protruding tire storage compartment designed to extend from the side of the cart, allowing for accessible and secure wheel placement.

[G3] Simple bucket style tire + rim holder.

[G4] Located in the largest bottom cabinet of the toolbox, this compartment offers significantly more space than other storage units, suitable for storing large items.